AD-A070 971 OWENS-ILLINOIS INC TOLEDO OH F/G 20/5
INVESTIGATION OF BROAD-BAND EMITTERS AS POTENTIAL LASING IONS B--ETC(U)
APR 79 C F RAPP, N L BOLING, C M CARLEN F44620-76-C-0088
UNCLASSIFIED AFOSR-TR-79-0736 NL

| OF |
AD
A070971

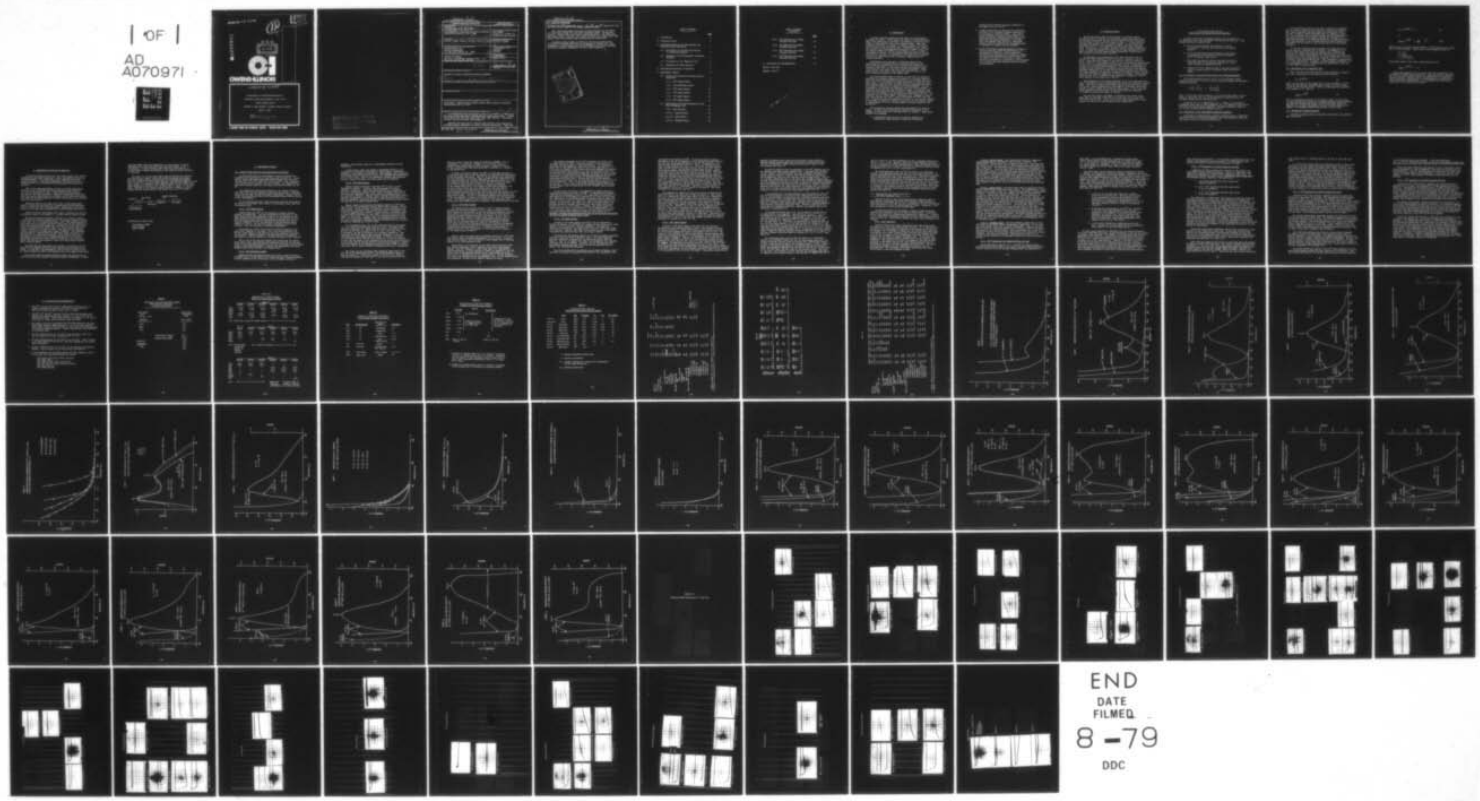

END
DATE
FILMED
8-79
DDC

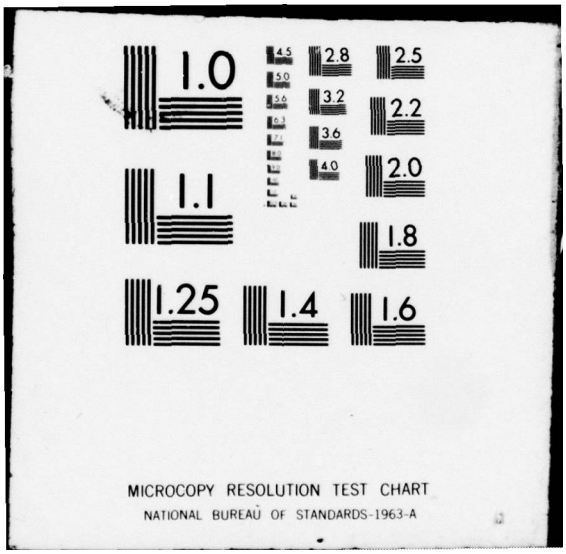
1.0
1.1
1.25
1.4
1.6
1.8
2.0
2.2
2.5
2.8
3.2
3.6
4.0
4.5
5.0
5.6
MICROCOPY RESOLUTION TEST CHART
NATIONAL BUREAU OF STANDARDS-1963-A

OWENS-ILLINOIS

F44620-76-C-0088

Investigation of Broad-Band Emitters As Potential Lasing Ions Between 0.5 and 1.0 μm

Final Progress Report

Charles F. Rapp, Norman L. Boling, Cloyce M. Carlen

April 2, 1979

A REPORT FROM THE TECHNICAL CENTER TOLEDO, OHIO, 43666

AIR FORCE OFFICE OF SCIENTIFIC RESEARCH (AFSC)
NOTICE OF TRANSMITTAL TO DDC
This technical report has been reviewed and is approved for public release IAW AFR 190-12 (7b).
Distribution is unlimited.
A. D. BLOSE
Technical Information Officer

Unclassified

SECURITY CLASSIFICATION OF THIS PAGE (When Data Entered)

REPORT DOCUMENTATION PAGE	READ INSTRUCTIONS BEFORE COMPLETING FORM
1. REPORT NUMBER: AFOSR-TR-79-0736	2. GOVT ACCESSION NO. / 3. RECIPIENT'S CATALOG NUMBER
4. TITLE (and Subtitle): Investigation of Broad-Band Emitters as Potential Lasing Ions Between 0.5 and 1.0 micrometers.	5. TYPE OF REPORT & PERIOD COVERED: Final Report. 76 June 01 - 78 Sept. 30
	6. PERFORMING ORG. REPORT NUMBER
7. AUTHOR(s): Charles F. Rapp, Norman L. Boling Cloyce M. Carlen	8. CONTRACT OR GRANT NUMBER(s): F44620-76-C-0088
9. PERFORMING ORGANIZATION NAME AND ADDRESS: Owens-Illinois, Inc. Corporate Technology P.O. Box 1035, Toledo, OH 43666	10. PROGRAM ELEMENT, PROJECT, TASK AREA & WORK UNIT NUMBERS: 61102F / 2301/A1
11. CONTROLLING OFFICE NAME AND ADDRESS: Director Of Physics Air Force of Scientific Research, Attn: N.D. Bldg. 410, Bolling AFB, DC 20332	12. REPORT DATE: April 2, 1979
	13. NUMBER OF PAGES: 77
14. MONITORING AGENCY NAME & ADDRESS (if different from Controlling Office): 77 p.	15. SECURITY CLASS. (of this report): Unclassified
	15a. DECLASSIFICATION/DOWNGRADING SCHEDULE

16. DISTRIBUTION STATEMENT (of this Report)

Approved for public release/distribution unlimited.

Final rept. 1 Jun 76 - 30 Sep 78,

17. DISTRIBUTION STATEMENT (of the abstract entered in Block 20, if different from Report)

18. SUPPLEMENTARY NOTES

19. KEY WORDS (Continue on reverse side if necessary and identify by block number)

Glass Lasers, Tunable Lasers, Visible Lasers, Near IR Lasers, Broad-Band Fluorescence, Eu^{2+}, Cu^{+}, Sn^{2+}

20. ABSTRACT (Continue on reverse side if necessary and identify by block number)

Ions exhibiting broad fluorescence bands in the 5000Å to 10,000Å region have been studied as potential lasing ions in various glass hosts. Included in the study were Eu^{2+}, Cu^{+}, Sn^{2+}, Sb^{2+}, Yb^{2+}, Ge^{2+}, and CdS. Glass hosts included silicates, borates, and phosphates.

Spectral data were used to calculate peak emission cross sections and flashlamp pumping thresholds for various ion-host combinations. These data

DD FORM 1 JAN 73 1473 EDITION OF 1 NOV 65 IS OBSOLETE

406 424

Unclassified

SECURITY CLASSIFICATION OF THIS PAGE (When Data Entered)

20. Abstract (continued)

indicated that Eu^{2+} should lase easily. Cu^{+}, Sn^{2+}, and Sb^{2+} should also lase but would require significantly greater pumping energies.

Gain (loss) measurements were made on selected glass rods by passing a CW laser beam through the rods during flashlamp pumping. No gain was measured. Instead, most rods showed a pumped absorption. This absorption was probably due to transient color center formation in the glass hosts themselves, rather than excited state absorption by the dopant ions.

Flashlamp pumping studies of several of the ions in various hosts selected for low pumped absorption is recommended as further work. Also recommended is laser pumping, which would eliminate the shorter wavelength ultraviolet primarily responsible for color center formation.

Table of Contents

Table of Contents
(continued)

A-043-145

1. Introduction

In recent years much effort has been spent on the development of organic dye lasers. These lasers are useful for many applications where other lasers are not because of the ability to select the wavelength of their emission over a wide spectral region. This wide wavelength selection, or "tuning", is possible because of the broad emission bands of the dyes being used. Unfortunately, most organic dyes undergo some photodecomposition when being "pumped" so that dye circulating systems are needed for the lasers, as well as regular replacement of the dye. If the problems associated with dye degradation could be overcome, the usefulness of the laser would be greatly increased for applications such as ranging, communications and isotope separation.

Approximately two years ago, a program was begun on the "Investigation of Broad-Band Emitters as Potential Lasing Ions". These broad band emitters were to be inorganic ions dispersed in an inorganic glassy host. It was hoped that in this program a solid state analog of the organic dye laser could be developed. If this could be done, this type of laser material should be free of the photo-instability problems of the organic dyes.

The broad emission bands of interest in this study are generally associated with allowed transitions as opposed to the narrow emission bands associated with forbidden transitions in the trivalent rare earth laser ions. It is desirable that these transitions be allowed so that their emission cross sections are large and their population inversions for threshold lasing are low, despite the large bandwidths. For the transitions to be allowed, the selection rule $\Delta\ell=\pm1$ must be obeyed. In surveying the various ions that fluoresce in glass, a relatively large number are found which meet this criterion. These ions generally fall into one of two classes: the rare earth ions displaying a $4f^{n-1}5d \rightarrow 4f^{n}$ transition and the "filled shell" fluorescent ions. Examples of ions in the first class are Ce^{3+}, Eu^{2+}, and in the second Tl^{+}, Pb^{2+}, Sb^{3+} and Sn^{2+}. While these ions emit anywhere from the UV to the infrared, interest in this study is limited to those ions which emit in the spectral region of approximately 0.5 to 1.0 μm (that region of primary interest to the Air Force).[1]

This exploratory research program was approximately two years in length. In order to most efficiently achieve the objectives of this program, it was divided into three major areas of activity. These areas included the following:

1. A literature survey was done in order to identify any glasses which might display a broad-band fluorescence

arising from an allowed electronic transition in the region of 0.5 to 1.0 μm.

2. A sample preparation and spectroscopic evaluation was done on the fluorescent glasses identified in the preliminary literature survey. This spectroscopic evaluation involved the measurement of the absorption spectra, emission spectra, fluorescent decay time and quantum efficiency. From these data, the emission cross section for stimulated emission could be calculated and the expected gain or threshold for lasing could be estimated.

3. Active lasing and/or gain measurements were made on the most promising candidates identified in the spectroscopic evaluation. These measurements included active lasing tests (an attempt to observe oscillation when the sample was placed between feedback mirrors) as well as active gain or pumped absorption measurements (a monitoring of the intensity of a cw probe laser beam passing through the sample during pumping).

2. Literature Survey

During the initial phase of this program, a literature survey was done in order to identify any fluorescent glasses that might display a broad-band fluorescence arising from an allowed electronic transition. The ions found in this survey are listed in Table I. In this table the ions have been divided into two general classes: the rare earth ions displaying a $4f^{n-1}5d \rightarrow 4f^n$ transition and the filled shell fluorescent ions. In addition, a fluorescent molecular species, cadmium sulfide, was found. Fluorescent glasses which were found but not included were those which contained ions displaying forbidden transitions (notably most of the trivalent rare earths, Mo^{3+} and Mn^{2+}).

As mentioned in the introduction, only those ions which emit in the spectral region between 0.5 and 1.0 μm are of interest to the Air Force. Those ions which seemed to fall within or near this region are given in Table II. Also listed in Table II are the electronic configurations of the ions, the approproximate color reported for their fluorescence and several of the most pertinent references. The 5,000 to 10,000Å region of interest was not considered too rigidly since the absorption and emission processes taking place in the ions involve bonding orbitals and, therefore, very large changes in the spectral locations of the emission bands can take place when the chemical composition of the host is changed. These changes can be of the order of hundreds or even thousands of angstroms. This is quite apparent in the cases of Cu^+ and Eu^{2+}.

This dependence of fluorescent wavelength on the host complicates the task of searching for ions to investigate for lasing in a particular spectral range. The task is further complicated by the broad emission bands, since an ion with a peak fluorescence at, say, 4500Å in a particular glass might be made to lase at 5500Å, if the band is broad enough. On the other hand, these complexities are beneficial in that they yield more candidates for lasing in a particular region of interest.

For the ions listed, the number of references found varied from a great many for the case of the Cu^+ ion to only one or two for the Ge^{2+}, Eu^{2+}, Yb^{2+}, and V^{5+} ions. Also, in the case of CdS, fluorescence in some glasses was reported but the activator was not identified.[1]

3. Calculations Used for the Spectroscopic and Potential Lasing Evaluation

In order to evaluate the lasing potential of a particular ion in a particular host, some "guideline" calculations are required. These calculations involve several steps:

a. Use of the spectroscopic data measured on the ion to calculate σ, the peak cross section for stimulated emission.

b. Use of the absorption spectra measured on the material to estimate ΔN, the population inversion obtainable with a "reasonable" pump source.

c. Use of the calculated σ and ΔN to further calculate an "expected" gain for the material when used in a laser under "reasonable" pumping conditions.

d. Comparison of this "expected" gain to the gain required for lasing, assuming some set of realistic laser cavity parameters.

3.1. Calculation of the Peak Cross Section for Stimulated Emission

The stimulated emission cross section σ for a potential lasing transition from level 2 to level 1 can be calculated through the Füchtbauer-Landenburg equation:

$$\sigma = \frac{1}{\tau_{21}} \frac{\lambda^2}{\pi \; 2 \; \Delta\nu} \quad \text{or} \quad \frac{1}{\tau_{21}} = \frac{\lambda^4}{n^2 \Delta\lambda 8\pi c}$$

where λ is the line center frequency, $\Delta\nu$ or $\Delta\lambda$ is the line width, n is the index of refraction, and $1/\tau_{21}$ is the spontaneous transition rate from the upper lasing level to the lower level.

To use Eq. (1) it is assumed that $\tau_{21} = \tau$, where τ is the measured fluorescent decay time or, more accurately, $\tau_{21} = \tau/\Phi$ where Φ is the quantum efficiency for the pertinent transition. The other parameters needed in Eq. (1) are obtained from the emission spectra.

3.2. Estimation of the "Obtainable" Population Inversion

An estimation of the population inversion obtainable with a "reasonable" pump source can be done from a knowledge of the ionic absorption bands and the spectral output of available pump sources.

If the absorption spectra of the ions of interest are examined, most are found to absorb in the ultraviolet region of the spectrum. Also, these absorptions generally appear as an absorption "edge". In order to define a useful wavelength region of pumping for these ions, it was assumed that effective pumping could be accomplished in the region where the optical density through the diameter of the laser rod was between 0.15 (≈30% absorption) and 1.8 (≈98% absorption). (Any light absorbed at a more intense absorption would primarily be concentrated at the surface of the rod and would not be efficiently utilized.)

To find the flashlamp energy available for pumping these ions, several realistic parameters can be assumed. For example, a 25 J pulse of light energy can easily be obtained from a 25,000°K lamp operating at a pulse length significantly shorter than 2 μsc (the shortest decay time ion found here). It can be formed from the 25,000°K black-body curve for such a lamp that about 18% of this 25 J, or 4.5 J, is emitted in the 2300-3600Å interval. This corresponds to approximately 0.35 J per 100Å interval. Assuming a rod-lamp coupling coefficient of 0.5, approximately 0.77 J of energy would be absorbed by a laser rod for each 100Å of pump band width.

3.3. Calculation of the "Expected" Gain

Once σ has been calculated and ΔN has been estimated, an expected gain can be calculated for the material from the equation:

$$G = e^{(\sigma \Delta N \ell - \alpha \ell)} \qquad (2)$$

where α is the loss per unit length and ℓ is the rod length. In this study this gain was not calculated since a value of α was not known for any of the materials tested. Rather, an ideal gain was calculated which assumes $\alpha = 0$. That is:

$$G_{ideal} = e^{\sigma \Delta N \ell} \qquad (3)$$

This is a meaningful quantity for two reasons first, it can be used to calculate the lasing threshold, assuming reasonable cavity parameters and loss coefficients; and second, it is the gain which should be observed in a cw laser beam passing through a rod when comparing the pumped to the unpumped condition (as was done in this study).

3.4. Estimation of Lasing Potential

In order to achieve lasing (a sustained oscillation), the condition must be met that:

$$r_1 r_2 \, e^{2\ell(\sigma\Delta N - \alpha)} \geq 1 \qquad (4)$$

or

$$G_{ideal} = e^{\sigma\Delta N \ell} \geq \frac{1}{r_1 r_2} \, e^{\alpha\ell} \qquad (4\text{-A})$$

where r_1 and r_2 are mirror reflectivities, α is the loss per unit length, and ℓ is the rod length. Typical laser cavity parameters might be:

$r_2 = 1.0$
$r_1 = 0.97$
$\alpha = 0.003 \text{ cm}^{-1}$
$\ell = 3" = 7.6 \text{ cm}$

Using these values in Eq. (4-A), lasing should occur if:

$$G_{ideal} = e^{\sigma\Delta N \ell} \geq 1.0$$

These calculations do not, of course, take into consideration the possibility of excited-state absorption. Since excited-state absorption can (and often does) prevent lasing, the possibility of its existence cannot be ignored. However, since it cannot generally be predicted from these spectroscopic measurements, it is considered later with active lasing tests in the material evaluations.

4. Experimental Evaluation of Materials

On selected samples prepared with the various dopant ions, various spectroscopic measurements were made. These measurements included the fluorescent decay time, absorption spectra, emission spectra and quantum efficiency. From these measurements the lasing potential for these materials can be calculated (as was discussed in the previous section).

Most of the above measurements are made by standard techniques. Since most ions of interest here have fluorescent decay times of a few tens of microseconds or less, a Xenon Corporation Micropulser was used for the flash excitation. Generally, appropriate narrow band pass filters were used between the flashlamp and the sample and between the sample and the photomultiplier in order to block any stray excitation light from the detector.

Absorption spectra were taken with a Cary 14 Spectrophotometer. Emission spectra were recorded with a scanning quartz prism monochronometer in conjunction with a photomultiplier. (Generally an S-20 type; however, an S-1 type can be substituted to extend further into the IR.)

Quantum efficiency measurements were made by comparing the relative fluorescence output of the samples to a quinine sulfate -H_2SO_4 solution.

The Lasing Evaluation Equipment consisted of an optical resonator, a flashlamp and an energy storage system. The optical resonator included a test laser rod, a 3% transmitting mirror, and a 100% reflecting mirror. These mirrors were purchased from Oriel Corporation and were specified to have broad band, multilayer dielectric coatings with "flat" reflectivity curves from 4500Å through 6500Å. They had a thirty-second wedge and a surface flatness of less than 1/10 wave. The laser rod was supported inside a four-inch arc length DL-10 coaxial flashlamp. This flashlamp was energized by a Phase-R Model DL-1100 power supply operating at 25 kilovolts and 0.3 microfareds producing a pulse width of less than 1 microsecond. The output of the transmitting mirror was observed by a Pin-10 diode detector from United Detector Technology. The electrical signal from this detector produced a trace on an oscilloscope equipped with a Polaroid camera.

The Laser Rod Gain Measurement test utilized a continuous wave (cw) laser and the flashlamp and power supply assembly from the pulsed laser system. In this test, the wavelength of the cw laser was chosen so that it closely matched the peak of the emission band of the sample being tested.

The cw laser beam was passed through the sample and was detected by a Pin-10 (silicon diode) detector from United Detector Technology. A narrow

band pass (NBP) filter was positioned over this detector to prevent extraneous light that would affect the electrical signal to the oscilloscope. A neutral density (ND) filter was also placed in the cw laser beam to reduce the intensity of the light and avoid saturation of the diode.

The 100% T or cw laser beam signal from the detector was traced on the oscilloscope's camera, along with the 0% T or blocked beam signal. Then the cw laser beam was recorded while the flashlamp was energized from a 25 kilovolt, 0.3 micro-farad capacitor from the Phase R-Model DL-1100 Laser System. An increase in this composite signal over the 100% T only signal signifies an adding to the cw laser beam, or a gain. On the other hand, a decrease in the composite signal indicates a pumped absorption, perhaps from the excited state of the dopant ion, in the test sample.

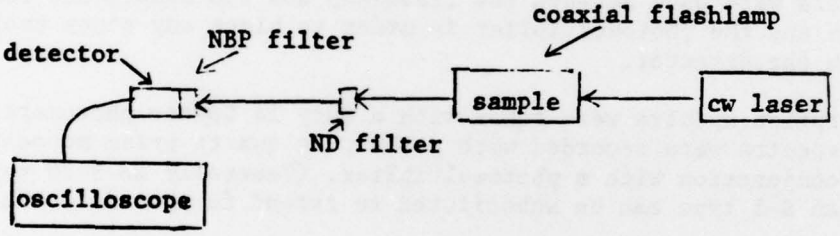

Continuous wave lasers used:

Helium-Neon (6328Å)
Argon (5017Å)
Argon (4545Å)

5. Experimental Results

5.1. Initial Glass Selection and Spectroscopic Evaluation

In the initial phase of this program, a series of glasses was prepared which contained most of the ions listed in Table II. In this series, several host glass compositions were selected and doped with the ions Cu^{+}, Ge^{2+}, Sn^{2+}, Sb^{3+}, Bi^{3+}, Eu^{2+} and Yb^{2+}. Also, commercial filter glasses which contained CdS were obtained. The compositions of some select glasses prepared in the study are listed in Tables III and IV.

In a preliminary qualitative examination, the glasses containing Cu^{+}, Sn^{2+}, Sb^{3+}, and Eu^{2+} appeared to show the most promise. Therefore, these ions have been the most thoroughly investigated. However, several of the other glasses have shown very interesting features and may warrant further investigation.

In the following sections, those ions which have been investigated the least and also appear least likely to be successful laser ions will be discussed first.

5.1.1. Ge^{2+} Doped Glasses

Glasses doped with Ge^{2+} can be produced by strongly reducing glasses containing GeO_2. This was accomplished in this study in the same manner as described elsewhere;[4] that is, by the addition of some glass constituents as acetates and melting in a covered SiO_2 crucible. Ge^{2+} was easily produced in the Na_2O-CaO-SiO_2 glass (AF-117) but, as reported elsewhere,[4] no Ge^{2+} was produced in the K_2O-BaO-GeO_2 glass without NiO (AF-127) but was in the glass containing a trace of NiO (AF-128). This is a puzzling but interesting phenomenon.

The production of Ge^{2+} could easily be detected visually by the yellow color imparted to the glass. Also, the red fluorescence from the Ge^{2+} could easily be seen when the glass was exposed to "long wave" UV excitation. However, because of the uncertainty in how much GeO_2 was reduced, it was not possible to estimate the amount of Ge^{2+} produced.

Ge^{2+} is one of the ions that appears very interesting for further study since it has a fluorescence that peaks well into the red and since it has a very broad absorption band in the blue (see Figure 1) which should result in very efficient pumping. However, the fluorescence does appear somewhat weak and may indicate a low quantum yield.

5.1.2. CdS Containing Glasses

Cadmium sulfide containing glasses can be made to absorb and emit throughout quite a large range in the visible and near-infrared, depending on their composition and the melting and heat-treatment conditions.

Therefore, these glasses could be of considerable interest for this application.

In this study, rather than expend a considerable effort on the development of preparation techniques for these glasses, commercially available filter glasses were purchased. These glasses show considerable fluorescence under UV excitation but were not evaluated spectroscopically due to lack of time. That is, the absorption, emission and excitation spectra, quantum efficiency, and decay times were not measured.

5.1.3. Yb^{2+} Doped Glasses

Several attempts were made to generate Yb^{2+} in Vycor, as was described by Wachtel.[10] However, this ion appeared to be quite difficult to generate. When using ytterbium nitrate to impregnate the Vycor, substantial amounts of Yb^{2+} could be produced only when the Vycor was also impregnated with large amounts of aluminum nitrate (as was reported by Wachtel). However, when a solution of ytterbium acetate was used to impregnate the "thirsty Vycor," and the sample fired in a 100% H_2 atmosphere, substantial amounts of Yb^{2+} could be generated without the addition of the extra aluminum salts.

Figure 2 shows the absorption and emission spectra of Yb^{2+} doped Vycor produced by impregnating "thirsty Vycor" with a solution of ytterbium acetate. (While the amount of reduction of the ytterbium was not quantitatively determined, this sample would contain 0.10 weight % YbO if all the ytterbium were reduced.) As can be seen, the emission peaks at about 5500Å and extends out past 7000Å. This is in about the ideal region for this study. However, most of the intense absorption of the Yb^{2+} is in the UV with a somewhat weak tail extending into the visible. This tail is apparently responsible for the excitation spectra (as shown by Wachtel) extending out to about 4500Å.

The fluorescence decay time of this glass was found to be 52 μsec, and the quantum efficiency was found to be about 7.2% under 2537Å excitation (see Table V). Using these two values, the radiative decay time for the Yb^{2+} was calculated to be 720 sec. This decay time is extremely long and is indicative of a forbidden transition. This transition may be the same as that which is responsible for the very weak absorption seen between 3000 and 5000Å. In order to calculate the fluorescence decay time for this transition, it would be necessary to know both the amount of Yb^{2+} generated and the nature (the multiplicity) of the ground and the excited states of the observed absorption. However, from the intensity of the absorption observed at about 3500Å, a fluorescent decay time of several hundred microseconds would not be unreasonable.

The reason for the relatively long fluorescent decay time of the Yb^{2+} ion is not immediately obvious. The expected emission would be from an allowed d → f transition, similar to the Eu^{2+} ion. However, this does not appear to be the case. It can only be speculated at this

time but it may be that the strong UV absorption (≈3000Å) is due to an allowed f → d transition. However, if a p orbital lies at a slightly lower energy than the upper d orbital, a decay from the d to the p orbital could take place producing a forbidden p → f emission to the ground state.

In order to determine whether the Yb^{2+} ion still has potential as a broad band laser ion, it will be necessary to determine the significance of the low quantum efficiency. That is, if the excited state responsible for the fluorescence is actually being quenched by some mechanism so that the radiative decay time is about 700 μsec (as calculated from τ/Φ), then the stimulated emission cross section for the Yb^{2+} ion would probably be too low to expect lasing to occur at a reasonable threshold. if the quantum efficiency is low because of some other mechanism, such as only a partial decay into this energy level, then the quantum efficiency from the fluorescent state itself may be nearer to 1.0 and the radiative decay time of this state may be near the measured 50 μsec. This radiative decay time would then give an emission cross section that might allow lasing. In order to distinguish between these possibilities, it will be necessary to measure the quantum efficiency of the fluorescent level. This might be done by direct excitation into the lower lying energy level with 3500Å radiation as opposed to the 2537Å radiation used here.

5.1.4. Eu^{2+} Doped Glasses

The absorption and emission spectra of Eu^{2+} in various silicate glasses have been given elsewhere,[1] but in order to generate Eu^{2+} in those glasses it was necessary to melt the glasses in graphite crucibles which reduced the glasses so severely that the glasses were somewhat darkened and showed considerable light scattering. But Eu^{2+} can be generated much more easily in "high silica" glasses (such as Vycor or fused silica) than it can be in more conventional silicate glasses. Almost all the europium doped into Vycor can be reduced to the Eu^{2+} state under quite mildly reducing conditions (10% H_2-90% N_2 atmosphere). (As a matter of fact, the blue Eu^{2+} fluorescence could be seen even in a sample which had been fired in air. It would be interesting to establish the $Eu^{2+} \rightleftarrows Eu^{2+}$ equilibrium in this material as a function of the oxygen partial pressure.)

Figure 3 shows the absorption and emission spectra of an Eu^{2+} doped "96% silica" glass containing approximately 0.02 wt. % EuO. As can be seen from the figures, this ion should be easily pumped with a flashlamp because of its broad absorption band.

Unfortunately, Eu^{2+} emission in this "96% silica" host is at somewhat shorter wavelengths than is desired for Air Force applications. However, since Eu^{2+} emission in other glass hosts is at considerably longer wavelengths, it may be possible to shift the emission in the "96% silica" host by impregnating "thirsty Vycor" with another ion at the same time it is impregnated with the europium salts. We have attempted to do this with aluminum nitrate and phosphoric acid, but the concentrations were apparently too high and the samples crumbled in firing.

The quantum efficiency of the Eu^{2+} fluorescence was found to be 0.77 when excited at 2537Å. This quantum yield is very high and is therefore very encouraging for laser applications. The fluorescent decay time of this sample was found to be 1.9 μsec (see Table V). If this value is corrected by the quantum efficiency (assuming the decrease in the quantum efficiency below 1.0 is due to nonradiative decay from the excited state) the radiative decay time for the Eu^{2+} ion is 2.5 μsec. If this value is combined with the emission wavelength and the emission band width, the peak cross section for stimulated emission can be calculated (see Section 3.1). This was done and the peak emission cross section for the Eu^{2+} ion in this host was found to be 8.65×10^{-20} cm^2 (see Table VI). This is a very high emission cross section for a glassy host. In fact, this cross section is approximately double that for the highest cross sections known for Nd^{2+} in glass (such as alkali phosphates).

As can be seen in Figure 3, the bandwidth for pumping this ion is quite broad--being on the order of 1440Å. If reasonably mild pumping conditions were considered, such as a 25 J pump pulse (see Section 3.2), approximately 2.5 joules should be absorbed by the laser rod (see Table VI). This would be a sufficient amount of energy to excite nearly all the Eu^{2+} ions in a 1/4" x 3" laser rod. Since it probably would not be possible to excite more than about 25 to 50% of the ions present, the maximum population inversion obtainable with this doping level would be about 0.5 to 1.0×10^{18} ions/cc. However, this should produce an "ideal" gain (no loss in the rod) for a 3" rod of approximately 1.4 to 1.9. This gain is much greater than the 1.04 which should be needed to produce lasing under reasonable conditions (see Section 3.4). Therefore, barring unpredictable factors such as excited state absorption, the Eu^{2+} ion should be easily made to lase.

5.1.5. Cu^{+} Doped Glasses

A series of Cu^{+} doped glasses (see Table III) was prepared by melting the glasses in a gas-fired pot furnace with an excess of CH_4 (with respect to air) to produce a reducing atmosphere. This was quite effective in reducing all the copper as no blue color (Cu^{2+}) was evident in the glasses. However, some light scatter could be seen in the sample, indicating the glasses may have been too strongly reduced.

The absorption and emission spectra of the the two glasses containing 0.05 mole % Cu_2O are shown in Figures 4 and 5. The light scattering mentioned previously is apparent in the absorption spectra shown in Figure 4. That is, it appears that there is an absorption tail extending throughout most of the visible. Actually, the Cu^{+} absorption in this glass should approach zero near 350 nm as does the spectrum shown in Figure 5 for the Na_2O-CaO-SiO_2 glass.

The areas obtained from the emission curves shown in Figures 4 and 5 were used to calculate the quantum efficiencies of the fluorescence when

the samples were excited at 2537Å. It was found that the quantum efficiency of the Cu^+ fluorescence in the Li_2O-CaO-SiO_2 glass (AF-110) was 0.61 and the quantum efficiency of the Cu^+ fluorescence in the Na_2O-CaO-SiO_2 glass (AF-104) was 0.67. Also, the fluorescent decay times of these glasses were found to be 32 sec for the Li_2O-CaO-SiO_2 glass (AF-110) and 27 for the Na_2O-CaO-SiO_2 glass (AF-104). Using the measured quantum efficiencies to correct these values, radiative decay times are 53 μsec for AF-110 and 41 μsec for AF-104. When these values are combined with the peak emission wavelengths and emission bandwidths, the peak cross sections for stimulated emission are found to be 0.34×10^{-20} cm^2 for AF-110 and 0.52×10^{-20} cm^2 for AF-104 (see Table VI). While these emission cross sections are much lower than that calculated for Eu^{2+} or those found for Nd^{3+} in glass, they are not greatly different than the emission cross sections for other known laser ions (such as Yb^{3+} in glass). Therefore, a cross section of this magnitude ($\approx 0.5 \times 10^{-20}$ cm^2) should not exclude Cu^+ from being considered as a potential laser ion.

The bandwidth for pumping the Cu^+ ion in AF-104 (a Na_2O-CaO-SiO_2 glass) was found to be about 320 to 340Å from Figure 5. This, along with a 25 J pump pulse, should yield about 0.55 to 0.59 J absorbed by the laser rod. This absorbed energy would be sufficient to produce a gain of approximately 1.014 in a 1/4" x 3" laser rod (see Table VI). This is well below the 1.04 gain estimated to be needed for lasing. Therefore, under these pumping conditions, lasing would not be expected from the Cu^+ ion. However, in a 3 mm x 3" rod, the expected gain would be 1.063, which is slightly above the 1.04 estimated gain for threshold. Therefore, lasing might be expected from Cu^+ in a 3 mm x 3" rod. This is particularly true for the pumping conditions used in the study where pump energies of about 94 J were used. This should have produced population inversions which were 6 times the expected threshold for lasing for a 3 mm x 3" rod, and even slightly exceeded the expected threshold for lasing for a 1/4" x 3" rod.

5.1.6. Sn^{2+} Doped Glasses

A series of Sn^{2+} doped glasses (see Table III) was prepared. The absorption and emission spectra of some of these glasses are shown in Figures 6 through 8. Under 2537Å excitation the quantum efficiency for the silicate glasses was found to vary between 0.12 and 0.47. The reason for this variation in quantum efficiencies becomes apparent when examining the absorption spectra of these glasses, and the undoped base glass, shown in Figure 6. That is, the absorption by the base glass is quite intense at 2537Å (1.30 cm^{-1}) and can effectively compete for the absorption of light with the Sn^{2+} ion in the more lightly doped glasses. For example, the absorption intensities are about 1.85 cm^{-1} and 5.78 cm^{-1} at 2537Å for the doped glasses containing 0.01 and 0.1 mole % SnO. Using these values and that of the undoped glass, the measured quantum efficiencies of the Sn^{2+} fluorescence can be corrected, giving 0.40 and 0.44 (as compared to 0.47 measured for the 1.0 mole % SnO glass). Using these values and the

measured fluorescent decay times (with excitation at about 2540Å and measured through a Schott BG18 green filter glass transmitting greater than 40% from ~3500Å to 6000Å) radiative decay rates of about 41 μsec are obtained (see Table V).

As might be expected from the appearance of the Sn^{2+} emission spectra, the emission from these glasses appears white. This seems very desirable for the "tunable" laser application since any wavelength throughout the visible might be selected. However, the band at 400 nm and the band at 600 nm apparently arise from two different initial energy levels. That is, in a previous unpublished work it was found that the 400 nm emission band is quite strong when the glass is excited at about 2500Å but nearly disappears from the emission spectrum when the glass is excited at longer UV wavelengths. While this phenomenon does complicate the estimation of the Sn^{2+} stimulated emission cross section and lasing potential, it probably does not produce a great error in these calculations since the long wavelength band appears to dominate the various spectroscopic measurements (peak λ, $\Delta\lambda$, τ).

It is possible that the same phenomenon is being observed in the Sn^{2+} ion in silicate glasses is the same as that taking place in the Cu^{+} ion. That is, the absorption is taking place in an allowed transition with short wave excitation. Direct emission from this level would be in the 400 nm band which may have a short decay time. However, most of the energy may decay to a slightly lower lying level which then has a forbidden transition and therefore a relatively long decay time. The 600 nm band would then result from the forbidden transition. However, the present data are not sufficient to establish this.

If the radiative decay time of 41 sec is taken for the Sn^{2+} ion in the glass AF119, a peak emission cross section of 0.45×10^{-20} cm^2 can be calculated for the 5850Å peak. This is nearly identical to that calculated for the Cu^{+} ion in the Na_2O-CaO-SiO_2 glass. It is also found that the bandwidth for pumping the Sn^{2+} ion is nearly the same as the Cu^{+} ion (see Table VI). Therefore, the possibility of lasing the Sn^{2+} ion in a silicate glass appears to be the same as that for lasing the Cu^{+} ion. That is, lasing might be expected for the Sn^{2+} ion in a 3 mm x 3" rod under reasonably low (25 J) pumping conditions but not in a 1/4" x 3" rod. However, under more intense pumping conditions (94 J), a population inversion approximately 6 times the expected threshold should be achieved for a 3 mm x 3" rod and near threshold conditions might be achieved for a 1/4" x 3" Sn^{2+} doped laser rod.

The fluorescent decay time for Sn^{2+} was found to be considerably shorter in the phosphate glass A123 than in the silicate glass A119. The quantum efficiency was also found to be about 22%. These values combine to give a radiative decay time in the phosphate glass of 26 μsec. However, because of the shorter wavelength of the emission peak in the phosphate glass, the stimulated emission cross section for the Sn^{2+} ion is only about $0.23 \times 10^{-20} cm^2$ (about one half that for the silicate glass). The effect of this lower cross section is nearly cancelled by the broader band width for pumping in the phosphate glass so that the gain is expected for the Sn^{+}

ion in a 3 mm x 3" rod under reasonably low (25 J) pumping conditions, but not in a 1/4" x 3" rod. However, under more intense pumping conditions (94 J), a population inversion approximately 7 times the expected threshold should be achieved for a 3 mm x 3" rod and near threshold conditions might be achieved for a 1/4" x 3" Sn^{2+} doped laser rod.

The fluorescent decay time for Sn^{2+} was found to be considerably shorter in the phosphate glass A123 than in the silicate glass A119. The quantum efficiency was also found to be about 22%. These values combine to give a radiative decay time in the phosphate glass of 26 μsec. However, because of the shorter wavelength of the emission peak in the phosphate glass, the stimulated emission cross section for the Sn^{2+} ion is only about $0.23 \times 10^{-20} cm^2$ (about one half that for the silicate glass). The effect of this lower cross section is nearly cancelled by the broader band width for pumping in the phosphate glass so that the expected gain for the Sn^{2+} ion is nearly identical in both the calcium phosphate and the Na_2O-SiO_2 glasses (see Table VI).

5.2. Spectroscopic and Laser Evaluation of the "Most Promising" Ions

From the results of the initial spectroscopic evaluation phase of this program, it appeared that three ions deserved further evaluation. These were the Eu^{2+}, Sn^{2+} and Cu^{+} ions. In addition, the Sb^{3+} ion appeared quite interesting in several glasses examined briefly. Therefore, it was also included as a fourth ion for further study.

In this second phase of the program, a series of glass melts were prepared which contained these four ions in various hosts. In addition, melts of the undoped base glasses were prepared for comparison. A listing of the compositions and melting conditions of these various glass melts is given in Table III. Spectroscopic samples and laser rods were prepared for testing.

5.2.1. Host Selection

Several different host glass compositions were used in this study. The objectives of this host variation were several: (1) to determine the variation in the spectroscopic properties of the dopant ions as the host was changed; (2) to eliminate or reduce the host excited state absorption or transient color center formation which occurred when pumping the laser rods; and (3) to improve the UV transparency of the host, which could increase the efficiency of pumping the dopant ions. It was found that changing the host composition had a marked effect on all three of these parameters. The effects on the first two parameters (the spectroscopic variation of the dopant ions and the color center formation) will be discussed in the later sections concerning individual ions. The effect on the third parameter, the UV transmission of the host, will be discussed here. For this study, host glass compositions were chosen from silicate, borate and phosphate systems.

5.2.1.1. Silicate Hosts - The silicate hosts used for doping were simple sodium-silicate containing a small amount of alumina. The compositions of these glasses can be formed in Table VII. Batch materials were chosen so that the iron level in these glasses should have been less than 10 ppm Fe_2O_3. The absorption spectra of several of these glasses are shown in Figure 9. As can be seen, there is essentially no difference in the absorption spectra of the Na_2O-SiO_2 glass and the Na_2O-CaO-SiO_2 glasses. The only spectrum which appears significantly different is that for the glass AF131-2. This glass was melted under reducing conditions so that most of the iron present in the glass is probably in the Fe^{2+} state rather than the Fe^{3+} state (Fe^{3+} absorbs in the UV while Fe^{2+} absorbs in the IR). This would tend to indicate that the UV absorption seen for the other three glasses in Figure VII is due to Fe^{3+} rather than the host absorption edge.

5.2.1.2. Borate Hosts - The borate hosts used for doping were either simple sodium borates or sodium calcium borates. The compositions of these glasses can be found in Table VII. Batch materials chosen for these glasses contained 3 ppm Fe_2O_3 in ine case (AF150-1 and AF151-1) and less than 0.3 ppm in a second ease (AF150-2 and AF151-2). (In the second set of glasses the iron level may have been much less than 0.3 ppm. However, the calorimetric test used for analyzing the boric acid used in these glasses was only sensitivie to 0.3 ppm Fe_2O_3. The sodium and calcium carbonates used contained less than 500 ppb Fe_2O_3.) The absorption spectra for these glasses are shown in Figures 10 and 11. As can be seen, there is a slight difference in the transmission for the 3 ppm and the <0.3 ppm melts. However, it was judged that this difference was slight so that the normal 3 ppm reagent grade batch materials were used for making the various doped samples. There is, however, a considerable difference between the Na_2O-B_2O_3 and the Na_2O-CaO-B_2O_3 transmissions. The simple Na_2O-B_2O_3 glasses were the most UV transparent glasses made in this study. Unfortunately, these glasses also had a very poor chemical durability, even showing some attack by atmospheric water.

5.2.1.3. Phosphate Hosts - The only phosphate glasses made in this study were of the simple calcium metaphosphate composition. It was hoped that these glasses would have a good UV transmission. However, as can be seen in Figure 12, this glass absorbed more strongly in the UV than either the borate or the silicate glasses. This may have been due to iron contamination from the melting crucible since these melts were made in alumina crucibles. This was not confirmed. (Melting could be done in a Pt crucible except dissolved Pt in phosphate glasses also absorbs strongly in the UV.)

5.2.2. Eu^{2+} Evaluation for Lasing Potential and Gain

As was discussed in Section 5.1.4., the Eu^{2+} ion should display a gain which should easily make it lase under reasonable pumping conditions. In fact, this ion is by far the most promising laser ion identified in

this study. It was estimated that a reasonably low pump energy (≈25 J) should produce a single pass gain in a 3" laser rod of about 1.4 to 1.9, which is at least ten times that which should be needed for lasing threshold. Therefore, a 4 mm x 3" laser rod was prepared for laser testing from an Eu^{2+} doped "96% silica" glass containing 0.02 wt. % EuO.

The above laser rod was tested for lasing as described in Section 4. However, no indication of lasing was observed. Therefore, the mirrors of the laser were removed and the rod was further tested for gain or excited state or other pumped abosrption by using a cw laser probe, as was also described in Section 4. The cw laser probe wavelengths used were 4545Å and 5017Å. The results of this test can be found in Appendix 1. As can be seen, rather than observing a gain in the intensity of the cw laser beam, a quite strong (>50%) absorption occurred in the rod under the flashlamp pumping. This absorption could be arising from several sources. The most likely of these are:

1. A loss of the cw probe laser light due to thermal distortion of the laser rod. (From the rapid decrease in the transmission, and from the intensity of the absorption, it is felt that a thermal distortion of the laser rod is probably not responsible for all of the absorption observed; however, it may be contributing some part.)

2. An excited state absorption in the Eu^{2+} ion. (Because of the long decay time observed for most of this absorption, it is probably not due to an excited state absorption in the Eu^{2+} ion. Any Eu^{2+} excited state absorption should have a very short decay time. However, the rapid decay time observed immediately after pumping could be due to this effect.)

3. A color center formation or trapped electron in the host. (Because of the long decay time of the absorption this appears to be the most likely effect.)

If color center formation is responsible for the observed absorption in the Eu^{2+} doped 96% SiO_2 glass, further development of the host may produce a successful laser material. For example, if the electrons which are producing the color centers in the glass arise from impurities such as Na^{+}, B^{3+}, Fe^{3+} etc., a pure fused silica host or CaF_2 host may be a successful candidate for an Eu^{2+} laser material. However, if the Eu^{2+} ion itself is acting as the source for the electrons forming the color centers, a proper host selection may not be sufficient for producing a successful host (such as the fused silica or CaF_2) and also use laser pumping directly into the longer wavelength Eu^{2+} absorption band for excitation. This would eliminate the harder UV which may be responsible for producing the

color centers in the material. It is strongly recommended here that these further investigations be pursued because of the high emission cross section of the Eu^{2+} ion and its great potential for lasing.

5.2.3. Cu^{+} Evaluation for Lasing Potential and Gain

A number of Cu^{+} doped glasses were prepared for this phase of the study under different melting conditions. Several of these melts were selected for preparation of spectroscopic samples and laser rods. The samples were selected from melts so that comparisons could be made among the different melting conditions. These melts were:

1. a Cu^{+} doped Na_2O-CaO-SiO_2 glass melted under reducing conditions
2. a Cu^{+} + Cu^{2+} doped Na_2O-CaO-SiO_2 glass melted in an air atmosphere
3. a Cu^{+} + Sn^{2+} doped Na_2O-CaO-SiO_2 glass melted in an air atmosphere

The first group of samples were clear glasses in which the copper was completely reduced to the Cu+ state. The second group of samples were from glasses which had a slight blueish color due to the Cu^{2+} present. The third group of samples were taken from a melt containing both Cu^{+} and Sn^{2+} ions. This melt was made in order to completely reduce the copper to the Cu^{+} state while melting in an air atmosphere (this is done by an internal oxidation of the Sn^{2+} during cooling). However, this melt partially "struck" to a ruby glass on cooling so that part of the melt was red and part was clear. The absorption and emission spectra of these glasses are shown in Figures 13, 14 and 15. As can be seen, the emission spectra of these several glasses are nearly identical. However, the absorption spectra do show characteristic differences. For example, the absorption producing the red color in the glass AF138-1 can be seen extending out past 600 nm. A Although not done in this study, it would be interesting to run an excitation spectra on this glass to determine if this absorption is effective for producing Cu^{+} fluorescence.

The various spectroscopic parameters measured and calculated for these glasses are also tabulated in Table VIII. As was found on the earlier melts of Cu^{+} containing glasses, the stimulated emission cross section for the Cu^{+} ion was found to be about 0.3 to 0.5 x $10^{-20}cm^2$. This emission cross section is sufficiently high to expect lasing under reasonable pump conditions (see Sections 5.1.5. and 3.4.).

Laser rods were prepared from several of these same melts and examined for gain or excited state absorption. The results or these tests are shown in Appendix 1. As can be seen, the glasses melted under both reducing and oxidizing conditions show very intense pumped absorptions throughout the visible region of the spectrum (6328Å, 5017Å and 4545Å). However, the glass melted with both Cu^{+} and Sn^{+} shows much less excited state absorption.

This could be due to a filtering effect of the Sn^{2+} or the copper ruby color.

It is felt that this excited state absorption is due to color center formation in the host rather than being characteristic of the Cu^{+} ion. The reasons for this opinion are several fold: first, the decay time of the Cu^{+} ion; second, the absorption is much too intense to be due to a thermal distortion of the laser rod (in fact the transmitted light through the laser rod can visually be seen to dim and then brighten again without a "blooming" of the beam); and third, the pumped absorption observed in undoped Na_2O-CaO-SiO_2 glasses is nearly the same in intensity and decay time as the Cu^{+} doped glasses (see the undoped glasses in Appendix I). Therefore, while the Cu^{+} ion does not have nearly as high an emission cross section as the Eu^{2+} ion, it is still an interesting and promising ion with respect to lasing. Therefore, experiments similar to those suggested for the Eu^{2+} ion would also be valuable for the Cu^{+} ion. That is, flashlamps and laser pumping of Cu^{+} doped fused silica or fluoride hosts is recommended.

5.2.4. Sn^{2+} Evaluation for Lasing Potential and Gain

A series of Sn^{2+} doped silicate, phosphate and borate glasses were prepared for this phase of the study. The compositions of these glasses are given in Table VII. The absorption and emission spectra of these glasses are shown in Figures 16 through 21. A very large shift in the emission peak to shorter wavelengths can be noted when going from the silicate to the phosphate and then the borate hosts. On closer inspection of the emission curves, the silicate and borate glasses may actually be quite similar where both contain a red and a blue band. However, in the silicate glass the red band is very intense, while in the borate glass it is very weak compared to the blue band. In the phosphate glass, only one band is evident.

The various spectroscopic parameters measured and calculated for these glasses are tabulated in Table VIII. The stimulated emission cross section for the Sn^{2+} ion was found to be about 0.4 to 0.5 x $10^{-20}cm^2$ in the phosphate and silicate glasses. For the borate glasses it was found to be somewhat lower, being about 0.25 to 0.3 x $10^{-20}cm^2$. This is primarily due to the shorter emission wavelength of the borate glasses. However, as was noted earlier, these cross sections and the resulting gains are sufficiently high to expect lasing under reasonable pump conditions.

Laser rods were prepared from several of these melts and examined for gain or excited state absorption. The results of these tests are shown in Appendix 1. As can be seen, the pumped absorptions of the silicate glasses were quite intense, especially at shorter wavelengths. However, they were not nearly as intense as those observed in the undoped or Cu^{+} doped silicate glasses. Since these decay times were also very long, it might be expected that these pumped absorptions were due to color center formation in the host (independent of the dopant ion).

The pumped absorptions observed in the Sn^{2+} doped phosphate and borate glasses were somewhat weaker than those observed in the silicates. Some were sufficiently weak so that thermal distortion may have been responsible

for the observed decrease in intensity. This was particularly true for the Sn^{2+} doped $CaO-P_2O_5$ glass and the Sn^{2+} doped $Na_2O-B_2O_3$ glass. However, this can not be stated with certainty without more extensive investigation.

Since some pumped absorption was observed in all of the samples tested, similar experiments to those recommended for the Eu^{2+} and Cu^{+} ions are also recommended here. That is, flashlamp and laser pumping of Sn^{2+} doped fused silica or fluoride crystals are recommended. In this case, however, laser pumping of the Sn^{2+} doped phosphate and borate glasses may also be worth pursuing.

5.2.5. Sb^{3+} Evaluation for Lasing Potential and Gain

A series of Sb^{3+} doped silicate, phosphate and borate glasses were prepared for this study. The compositions of these glasses are given in Table VII. The absorption and emission spectra of these glasses are shown in Figures 22 through 25. As in the case of the Sn^{2+} ion, quite large shifts are found for the peak emission wavelength when the host glass is varied. However, unlike the other ions examined, a very large host dependence of the quantum efficiency of the Sb^{3+} fluorescence was found. In fact, the quantum efficiency of the Sb^{3+} ion in the borate hosts was so low that these glasses should probably not be considered as potential laser materials.

The various spectroscopic parameters measured and calculated for the various Sb^{3+} doped glasses are given in Table VIII. The stimulated emission cross section for the Sb^{3+} ion was found to be about 0.4 and 0.6 x $10^{-20}cm^2$ in the silicate and phosphate hosts respectively. These cross sections are very nearly the same as those calculated for the Sn^{2+} and Cu^{+} doped glasses. Therefore, these Sb^{3+} doped glasses might be considered to have about the same lasing potential as the Sn^{2+} and Cu^{+} doped glasses.

Laser rods prepared from several of these melts were examined for gain or excited state absorption. The results of these tests are shown in Appendix 1. The pumped absorption observed in the Sb^{3+} doped silicate glass was sufficiently intense that it is felt that it is similar in nature to that observed in the other various silicate glasses tested. However, very little if any excited state absorption can be seen in the Sb^{3+} doped $CaO-P_2O_5$ glass tested. This observation, along with the reasonably high emission cross section (0.6 x $10^{-20}cm^2$) and the high expected gain under pumping conditions (see Table VIII), make this a promising candidate for further testing. In addition, a similar recommendation as was made for the several other ions is made here. That is, flashlamp and laser pumping of Sb^{3+} doped fused silica or fluoride crystals is recommended.

6. Conclusions and Recommendations

1. The Eu^{2+} ion was found to have a peak emission cross section for stimulated emission of about $9 \times 10^{-20} cm^2$ in a 96% SiO_2 host. This is very high and should easily lead to lasing.

2. The Cu^{+}, Sn^{2+} and Sb^{2+} ions were found to have peak emission cross sections for stimulated emission of about 0.4 to $0.5 \times 10^{-20} cm^2$ in various glass hosts. These cross sections are somewhat low but should still lead to lasing under reasonable pump conditions.

3. No lasing or net gain was observed for any glass tested in this study. Most glasses showed a pumped absorption. It is felt that transient color center formation (solarization) in the glass host itself produced the observed pumped absorptions. (Rather than excited state absorption in the dopant ions.)

4. The most promising host for the Eu^{2+} ion is 96% SiO_2 or 100% SiO_2. This is based on the ease of reducing Eu^{2+} to Eu^{2+}.)

5. The most promising host for the Sb^{2+} ion is $CaO \cdot P_2O_5$. (This is based on the high emission cross section, efficient pumping and low excited state absorption.)

6. The most promising hosts for the Sn^{2+} ion were $CaO \cdot P_2O_5$ and Na_2O-B_2O_3 glasses. (This is based on low excited state absorptions.)

7. It is recommended that flashlamp pumping and laser pumping be used to further test the following materials for lasing:

   Eu^{2+} doped fused silica (first priority)
   Eu^{2+} doped CaF_2.
   Cu^{+}, Sn^{2+} and Sb^{3+} doped fused silica
   Cu^{+}, Sn^{2+} and Sb^{3+} doped fluoride crystals.
   Sb^{3+} doped $CaO \cdot P_2O_5$
   Sn^{2+} doped $CaO \cdot P_2O_5$

Table I

Fluorescent Ions in Glass Which Display High Oscillator Strengths (Allowed Transitions)

Rare Earths with $4f^{N-1}5d \rightarrow 4f^{N}$ Emission		Filled Shell Fluorescent Ions (S^2 or d^{10})
Ce^{3+}		Tl^{+}
$*Eu^{2+}$		Pb^{+}
Yb^{2+}		Ag^{+}
	Fluorescence Greater Greater Than 5000Å	$*Cu^{+}$
		$*Sn^{2+}$
Molecular		Sb^{3+}
Suspension		Ge^{2+}
CdS		Bi^{3+}
		V^{5+}

Table III

Compositions of Select Glasses
Melted for Spectroscopic Studies

	Weight %					
	AF-103	AF-104	AF-105	AF-109	AF-110	AF-111
SiO_2	73.30	73.27	73.30	68.77	68.74	68.76
Al_2O_3	1.69	1.69	1.69	4.86	4.86	4.86
Li_2O	-	-	-	15.67	15.66	
Na_2O	13.50	13.49	13.50	-	-	-
CaO	11.50	11.50	11.50	10.70	10.69	10.70
Cu_2O	-	0.05	0.01	-	0.05	0.01
Atm:	Excess CH_4 in gas-air fired furnace ⟶					

	Wt. %	Mole %				
	AF-117	AF-118	AF-119	AF-120	AF-121	AF-122
SiO_2	50.0	75.0	75.0	75.0	75.0	75.0
Na_2O	22.0	25.0	25.0	25.0	25.0	25.0
CaO	8.0	-	-	-	-	-
GeO_2	20.0	-	-	-	-	-
SnO	-	-	0.01	00.1	1.0	-
Sb_2O_3	-	-	-	-	-	0.1
Atm:	sodium added as acetate-melted in covered crucible	Air in Electric Furnace ⟶				

	Mole %					
	AF-123	AF-124	AF-125	AF-126	AF-127	AF-128
CaO	50.0	50.0	50.0	-	-	-
P_2O_5	50.0	50.0	50.0	-	-	-
K_2O	-	-	-	17.0	17.0	17.0
BaO	-	-	-	17.0	17.0	17.0
GeO_2	-	-	-	66.0	66.0	66.0
SnO	0.1	-	-	-	-	-
Sb_2O_3	-	00.1	-	-	-	-
Bi_2O_3	-	-	0.1	-	-	-
NiO	-	-	-	-	-	0.01
Atm:	air ⟶			made from carbonate constituents	K and Ba added as acetates - melted in covered crucible	

Table II

Dopants in Glass which Fluoresce at Wavelengths Greater Than 5000 Å

Ion	Configuration	Fluorescence color	Reference
Cu^{+}	d^{10}	blue-green	3, 6
Ge^{2+}	s^2	orange-red	4
Sn^{2+}	s^2	white	5, 6
Sb^{3+}	s^2	whitish-blue	5, 6
Bi^{3+}	s^2	blue (narrow red?)	6, 11
V^{5+}	rare gas	yellow	7
CdS	molecule	variable thru vis. and IR	8, 9
Eu^{2+}	rare earth	blue to green	1, 2, 10
Yb^{2+}	rare earth	green	10

Table IV

Compositions of Vycor Doped Samples Prepared for Spectroscopic Studies

	Wt. % 7414-8G*		7414-114A**
SiO_2	96.3	(by difference)	
Na_2O	0.025	chemical analysis of commercial Vycor (96% SiO_2)	Nominally the same as 7414-8G. However, was not analyzed and was a different lot of Vycor.
Al_2O_3	0.32		
B_2O_3	3.34		
Fe_2O_3	0.004		
EuO	0.02		--
YbO	--		0.10
Atm:	fused in 10% H_2 - 90% N_2		fused in 100% H_2

* Prepared by soaking porous Vycor in a solution containing 0.00187 g of $Eu(NO_3)_3 \cdot 6H_2O$ per cc of solution. Concentration was chosen so that absorbance would be about 4/cm at peak of Eu^{2+} absorption according to data of J. H. Macky and J. Nahum.

** Prepared by soaking porous Vycor in a solution containing 0.0037 g Yb_2O_3 per cc of solution as ytterbium acetate.

Table V

Fluorescent Decay Time and Quantum Efficiencies of Select Glasses

	Host	Ion	τ (μsec)	ϕ	ϕ^*	τ_{21} (μsec)
7414-8G	Vycor	Eu^{2+}	1.9	0.77	--	2.5
7414-114A	Vycor	Yb^{2+}	52.0	0.072	--	720
AF-119	Na_2O-SiO_2	Sn^{2+}	16.3	0.12	0.40	41
AF-120	Na_2O-SiO_2	Sn^{2+}	19.1	0.34	0.44	43
AF-121	Na_2O-SiO_2	Sn^{2+}	19.0	0.47	0.47	40
AF-123	CaO-P_2O_5	Sn^{2+}	5.8	0.22	--	26
AF-110	Li_2O-CaO-SiO_2	Cu^+	32.4	0.61	--	53
AF-111	Li_2O-CaO-SiO_2	Cu^+	33.1	--	--	
AF-104	Na_2O-CaO-SiO_2	Cu^+	27.2	0.67	--	41
AF-105	Na_2O-CaO-SiO_2	Cu^+	29.4	--	--	
AF-122	Na_2O-SiO_2	Sb^{3+}	9.6			

τ = measured fluorescent decay time

ϕ = quantum efficiencies

ϕ^* = quantum efficiencies corrected for interference by base glass absorption

τ_{21} = radiative decay time

Table VI

	AF119	AF123	AF104	AF110	7414-8G	
Dopant Ion	Sn^{2+}	Sn^{2+}	Cu^{+}	Cu^{+}	Eu^{2+} →	≈ 2 x 10^{18} ions/cc
Glass Type	Na-Si	Ca-P	Na-Ca-Si	Li-Ca-Si	96% SiO_2	
nλ (Estimated)≈	1.50	1.51	1.52	1.53	1.48	
Emission: τ(10^{-6} sec)	16.3	5.8	27.2	32.4	1.9	
ϕ	(0.40)	0.22	0.67	0.61	0.77	
τ_{21} (=τ/ϕ)(10^{-6} sec)	(41)	26	41	53	2.5	
Peak λ (Å)	(1.0(0.68) 3900, 5850	4090	5030	4700	4850	
$\Delta\lambda$ (Å)(FWHM)	3100	2240	1580	1450	1370	
Effective $\Delta\lambda$(Å)	2550	2690	1730	1540	1550	
σ (10^{-20} cm^2)	0.13, 0.45	0.23	0.52	0.34	8.65	
Pump Band*: For 1/4" rod:	AF121					
$\Delta\lambda$(Å)	260	520	320		1440	
Center of band (Å)	2990	2940	2940		2990	
For 3 mm rod:						
$\Delta\lambda$(Å)	320	540	340		1440	
Center of band (Å)	2880	2790	2820		2990	
Useful E Absorbed**: For 1/2" rod:						
E absorbed (J)	0.45	0.90	0.55		2.49	Therefore, maximum would
# of photons (x 10^{17})	6.79	13.3	8.15		37.6	be about:
ΔN (ions/cc)(x 10^{18})	0.28	0.55	0.34		1.56 →	0.5 to 1.0
exp ($\sigma\Delta N\ell$)(3" rod)	1.010	1.010	1.014		2.80 →	1.4 to 1.9
For 3 mm rod:						
E absorbed (J)	0.55	0.93	0.59			
# of photons (x 10^{17})	7.96	13.1	8.37			
N(ions/cc) (x 10^{18})	1.47	2.43	1.55			
exp ($\sigma\Delta N\ell$)(3"rod)	1.052	1.044	1.063			

* Assuming a minimum O.D. of 0.15 and a maximum O.D. of 1.8 through the rod.

** Assuming a 25 J pump pulse with 18%, or 4.5 emitted between 2300 and 3600Å; and a 50% coupling coefficient into the rod.

Table VII

Weight %

	AF129	AF130	AF131	AF132	AF133	AF134	AF135	AF136	AF137	AF138
SiO_2	73.3	73.3	73.3	68.77	68.77	68.77	73.3	73.3	73.3	73.3
Al_2O_3	1.7	1.7	1.7	4.86	4.86	4.86	1.7	1.7	1.7	1.7
Li_2O	-	-	-	15.67	15.67	15.67				
Na_2O	13.5	13.5	13.5	-	-	-	13.5	13.5	13.5	13.5
CaO	11.5	11.5	11.5	10.70	10.70	10.70	11.5	11.5	11.5	11.5
SnO							-	0.22	-	0.22
Cu_2O	0.05	0.01	-	0.05	0.01	-	-	-	0.05	0.05
Atm:	Excess CH in gas-air fired furnace →						Air in electric furnace →			

Mole %

	AF139	AF140	AF141	AF142	AF143	AF144	AF145	AF146	AF147	AF148	AF149
SiO_2	73.51	75.0	75.0				73.51	73.51	-	-	-
Al_2O_3	1.00	-	-				1.00	1.00	-	-	-
Na_2O	13.13	25.0	25.0				13.13	13.13	-	-	-
CaO	12.36	-	-	50.0	50.00	50.0	12.36	12.36	50.0	50.0	50.0
P_2O_5	-	-	-	50.0	50.0	50.0	-	-	50.0	50.0	50.0
Sb_2O_3							-	0.5	-	0.5	-
SnO_2	0.50	-	0.5	-	0.1	0.5	-	-	-	-	0.5
Atm:	Air in electric furnace →										

	AF150	AF151	AF152	AF153	AF154	AF155
B_2O_3	84.0	74.0	84.0	84.0	74.0	74.0
Na_2O	16.0	16.0	16.0	16.0	16.0	16.0
CaO	-	10.0	-	-	10.0	10.0
SnO	-	-	0.5	-	0.5	-
Sb_2O_3	-	-	-	0.5	-	0.5
Atm:	Air in electric furnace →					

Table VIII.

	AF146-1	AF148-1	AF153-1	AF155-1	AF141-1	AF139-1	AF144-1	AF149-1	AF152-1	AF154-1	AF129-2	AF137-1	AF138-1
Dopant Ion	Sb^{3+}	Sb^{3+}	Sb^{3+}	Sb^{3+}	Sn^{2+}	Sn^{2+}	Sn^{2+}	Sn^{2+}	Sn^{2+}	Sn^{2+}	Cu^{+}	Cu^{+}	$Co^{+} + Sn^{2+}$
Glass Type	Na-Ca-Si	Ca-P	Na-B	Na-Ca-B	Na-Si	Na-Ca-Si	Ca-P	Ca-P	Na-B	Na-Ca-B	Na-Ca-Si	Na-Ca-Si	Na-Ca-Si
n_R (Estimated)	1.52	1.51	1.48	1.50	1.50	1.52	1.51	1.51	1.48	1.50	1.52	1.52	1.52
Emission: $\tau(10^{-6}$ sec)	6.6	5.0	(0.48)	(5.4)	20.8	17.6	9.6	6.4	8.9	10.5	31.6	32	30(29.5)
ϕ	0.36	0.28	(0.05)	(0.06)	0.38	0.46	0.46	0.17(0.25)	0.67	0.62	0.65	0.45	0.22(0.53)
$\tau_{21}(=\tau/\phi)(10^{-6}$ sec)	18.3	17.9	(9.6)	(90.0)	54.7	38.3	20.9	37.6(25.6)	13.3	16.9	48.6	71.1	136(55.7)
Peak λ (Å)	3780	4450	6810	3730	6390	5930	4310	4420	3220	3630	5050	5030	5050
$\Delta\lambda$(Å)(FWHM)	1280	2220	(3760)	2880	3880	4380	2330	2250	1570	1920	1500	1510	1630
Effective $\Delta\lambda$ (Å)	1740	2250	-	2620	3710	3990	2310	2270	1700	2350	1610	1610	1800
$\sigma(10^{-20}$ cm^2)	0.37	0.57			0.48	0.46	0.42	0.26(0.38)	0.29	0.26	0.48	0.32	0.15(0.37)
Pump Band*: For 1/4" rod:													
$\Delta\lambda$(Å)	225	460			500	270	610	610	290	320	380	360	410
center of band (Å)	3020	3070			3130	2970	2930	2950	2870	2890	2890	3010	3040
For 3 mm rod:									440				
$\Delta\lambda$(Å)	375	480			380	300	690	900	440	600	410	380	420
Center of band (Å)	2900	2930			2970	2840	2740	2650	2730	2640	2760	2880	2880
Useful E Absorbed**: For 1/4" rod:													
E absorbed (J)	0.39	0.80			0.87	0.47	1.06	1.06	0.50	0.55	0.66	0.62	0.71
# of photons ($\times 10^{16}$)	5.94	12.3			13.7	7.03	15.7	15.8	7.24	8.01	9.61	9.39	10.9
ΔN(ions/cc)($\times 10^{18}$)	0.25	0.51			0.57	0.29	0.65	0.66	0.30	0.33	0.40	0.39	0.45
exp ($\sigma\Delta N\ell$)(3" rod)	1.007	1.022			1.021	1.010	1.021	1.013(1.019)	1.007	1.007	1.015	1.010	1.005(1.013)
For 3 mm rod:													
E absorbed (J)	0.65	0.83			0.66	0.52	1.19	1.56	0.76	1.04	0.71	0.66	0.73
E of photons ($\times 10^{17}$)	9.49	12.3			9.87	7.44	16.4	20.9	10.5	13.8	9.86	9.57	10.6
ΔN(ions/cc)($\times 10^{18}$)	1.76	2.28			1.83	1.38	3.04	3.87	1.94	2.56	1.83	1.77	1.96
exp($\sigma\Delta N\ell$)(3"rod)	1.051	1.104			1.069	1.050	1.10	1.08(1.12)	1.044	1.052	1.069	1.044	1.023(1.057)

* Assuming a minimum O.D. of 0.15 and a maximum O.D. of 1.8 through the rod.

** Assuming a 25 J pump pulse with 18%, or 4.5 J emitted between 2300 and 3600Å; and a 50% coupling coefficient into the rod.

FIGURE 1

ABSORPTION SPECTRA FOR GERMANIUM CONTAINING GLASS.

AF-117-1 MELTED IN AIR USING CARBONATE CONSTITUENTS,
AF-117-2 MELTED IN COVERED CRUCIBLE WITH Na ADDED
AS ACETATE TO REDUCE Ge

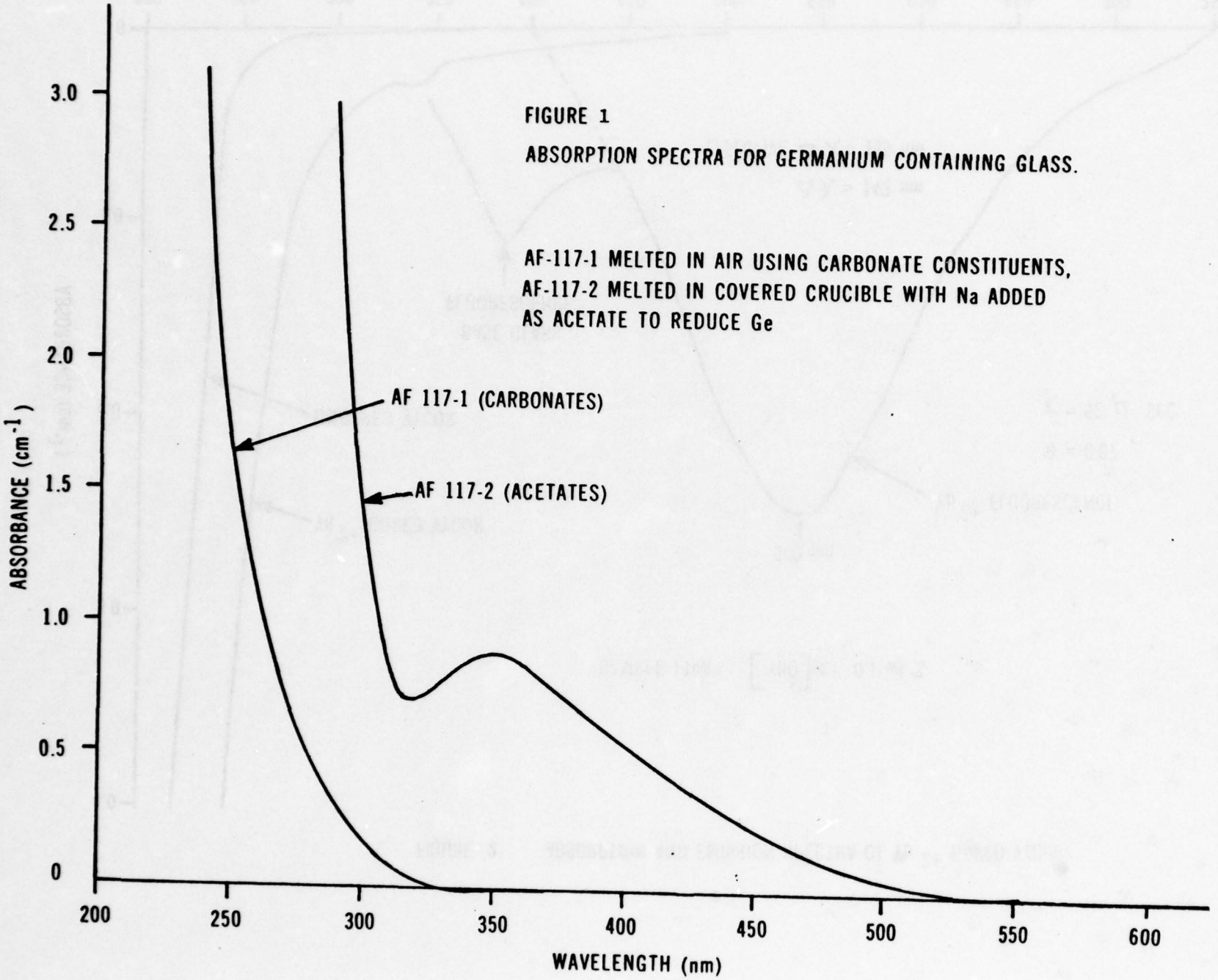

FIGURE 2 ABSORPTION AND EMISSION SPECTRA OF Yb^{2+} DOPED VYCOR

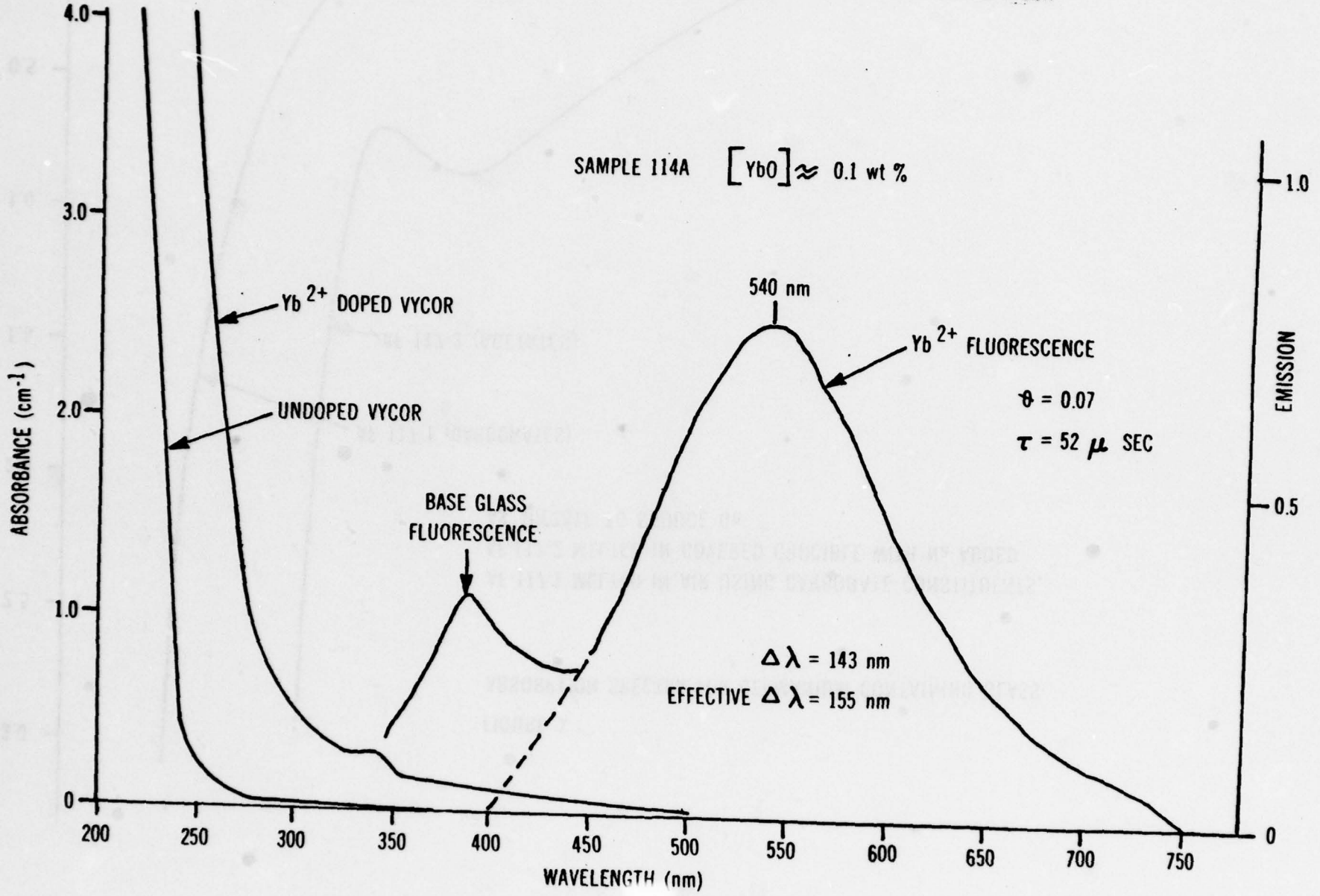

Figure 3 ABSORPTION AND EMISSION SPECTRA OF EUROPIUM DOPED VYCOR (GLASS 7414-8G OF TABLE 2).

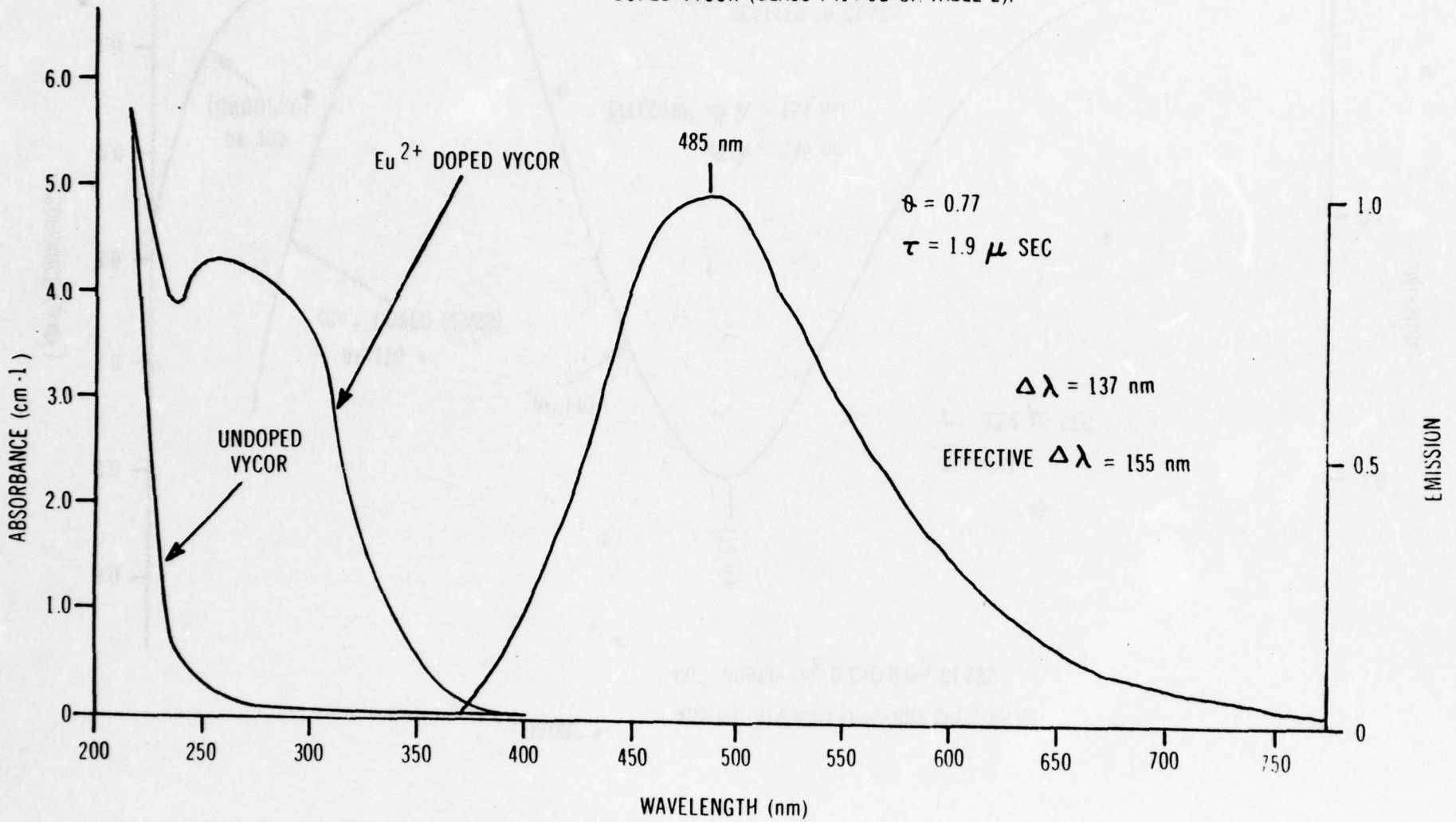

FIGURE 4.

ABSORPTION AND EMISSION SPECTRA OF
Cu^{+} DOPED Li_2O-CaO-SiO_2 GLASS.

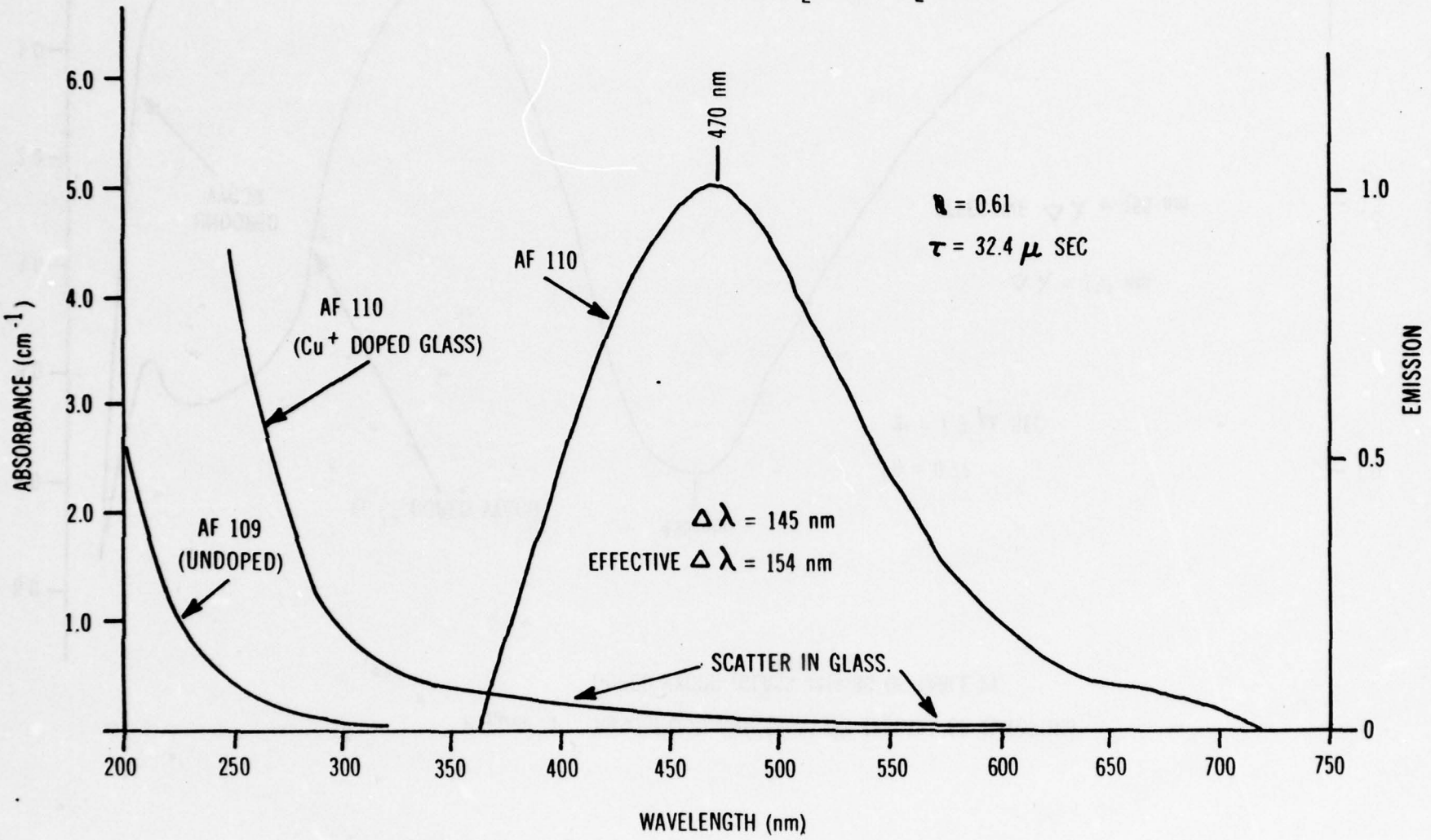

FIGURE 5. ABSORPTION AND EMISSION SPECTRA FOR Cu^{+} DOPED Na_2O-CaO-SiO_2 GLASSES.

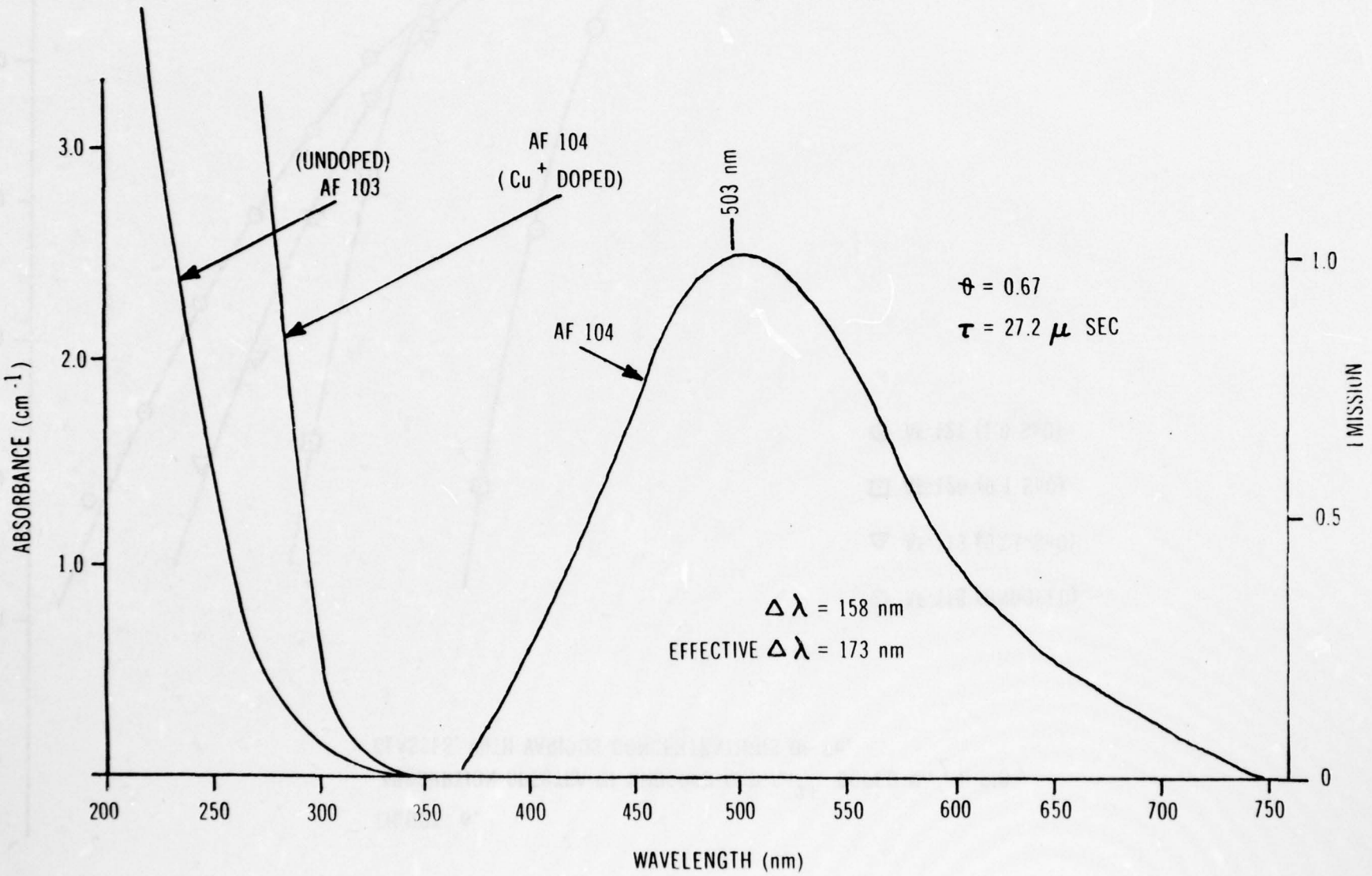

FIGURE 6.

ABSORPTION SPECTRA OF UNDOPED AND Sn^{2+} DOPED Na_2O-SiO_2 GLASSES, WITH VARIOUS CONCENTRATIONS OF Sn.

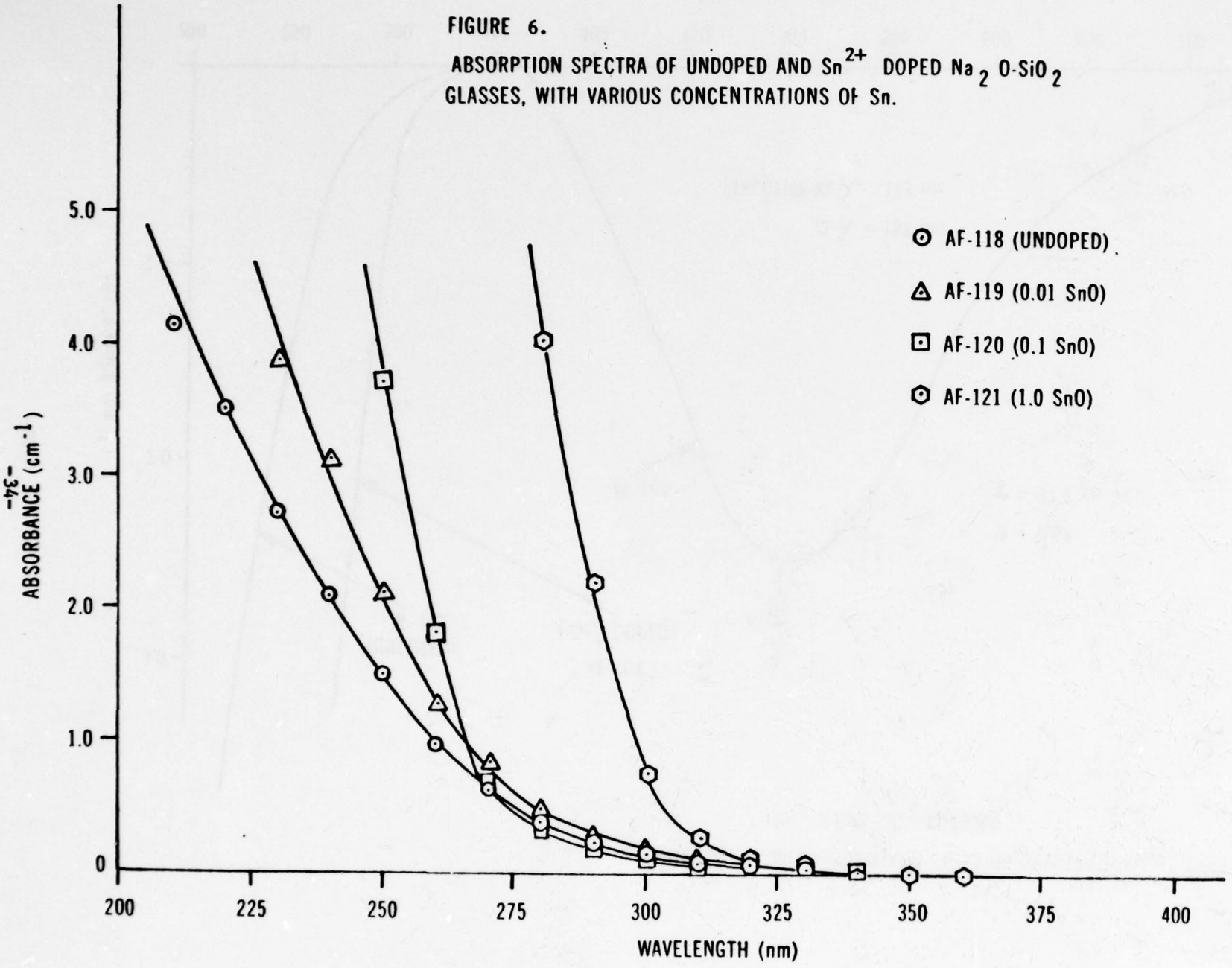

FIGURE 7. EMISSION SPECTRA OF Sn^{2+} IN $Na_2O \cdot 3SiO_2$ GLASSES WITH VARIOUS CONCENTRATIONS OF Sn.

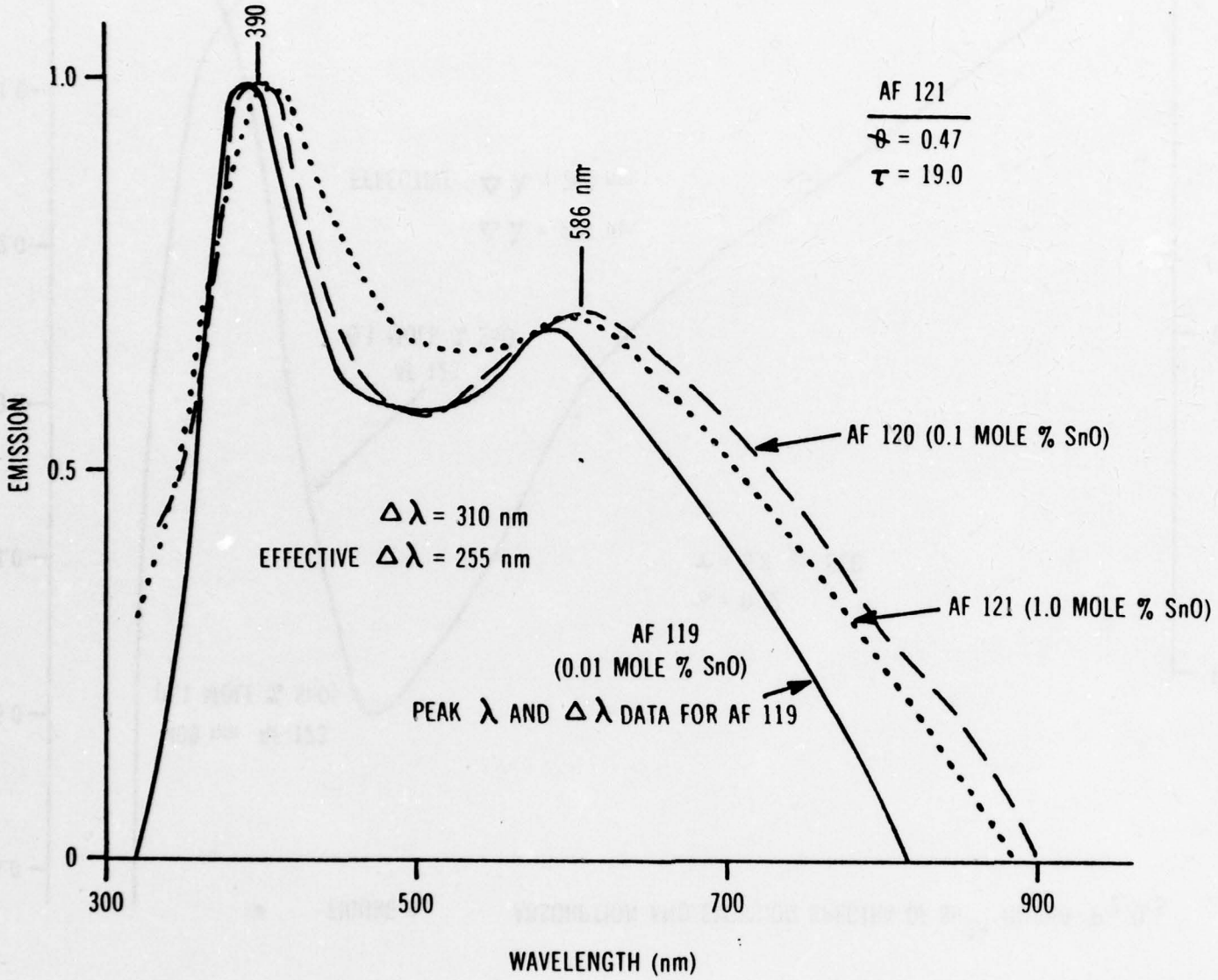

FIGURE 8. ABSORPTION AND EMISSION SPECTRA OF Sn^{2+} IN $CaO \cdot P_2O_5$

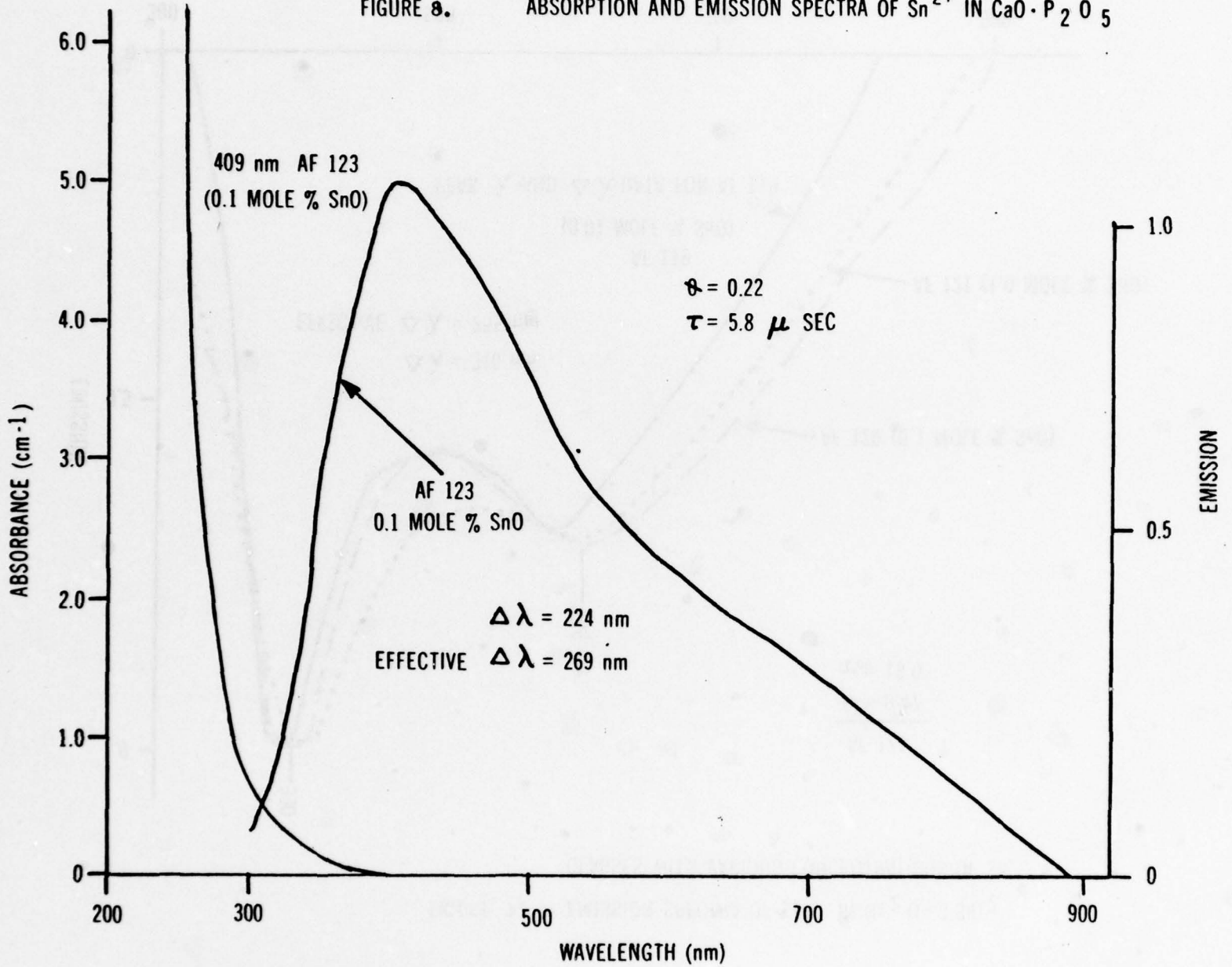

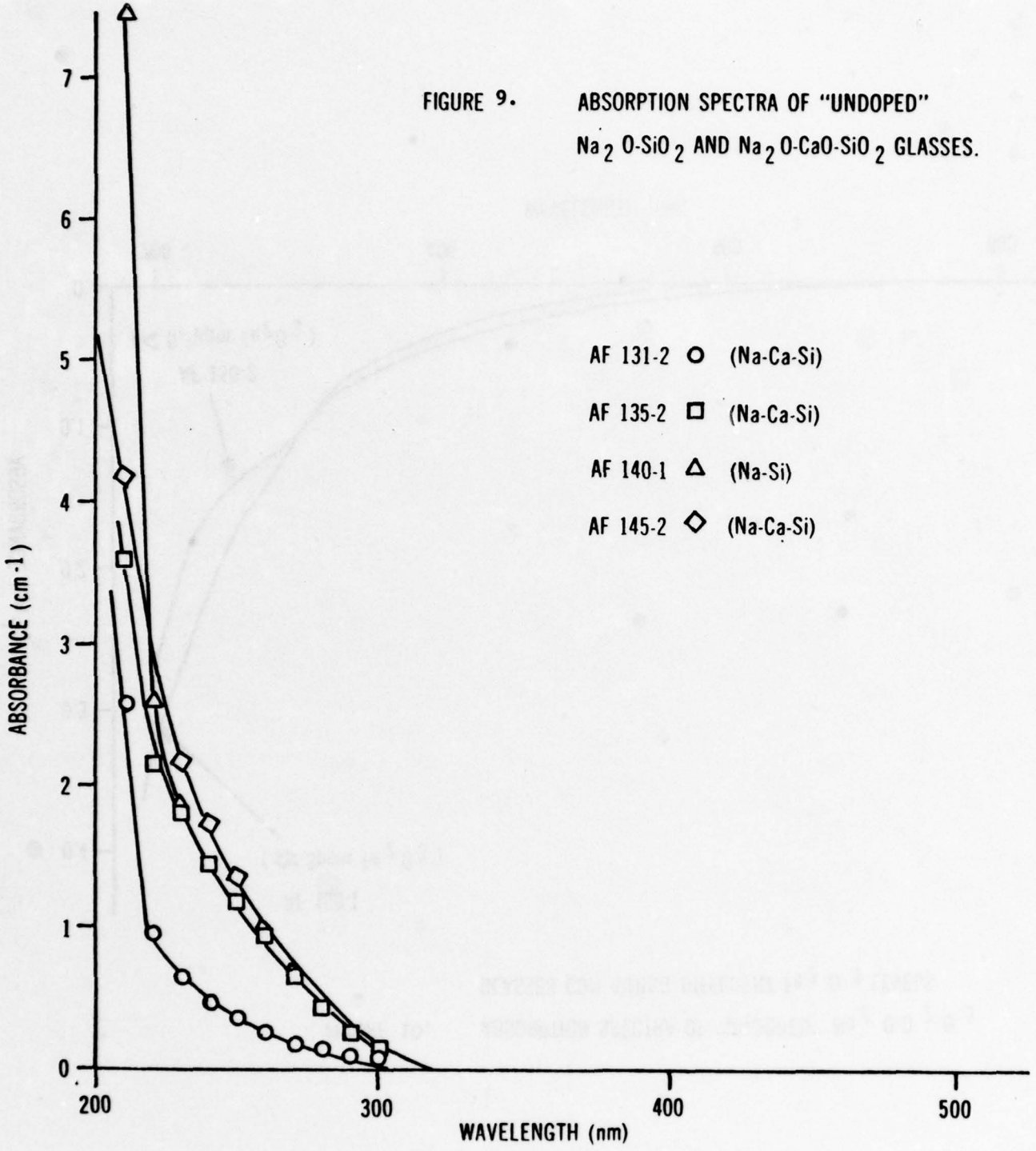

FIGURE 9. ABSORPTION SPECTRA OF "UNDOPED" Na_2O-SiO_2 AND Na_2O-CaO-SiO_2 GLASSES.

FIGURE 10. ABSORPTION SPECTRA OF "UNDOPED" Na_2O-B_2O_3 GLASSES CONTAINING DIFFERENT Fe_2O_3 LEVELS.

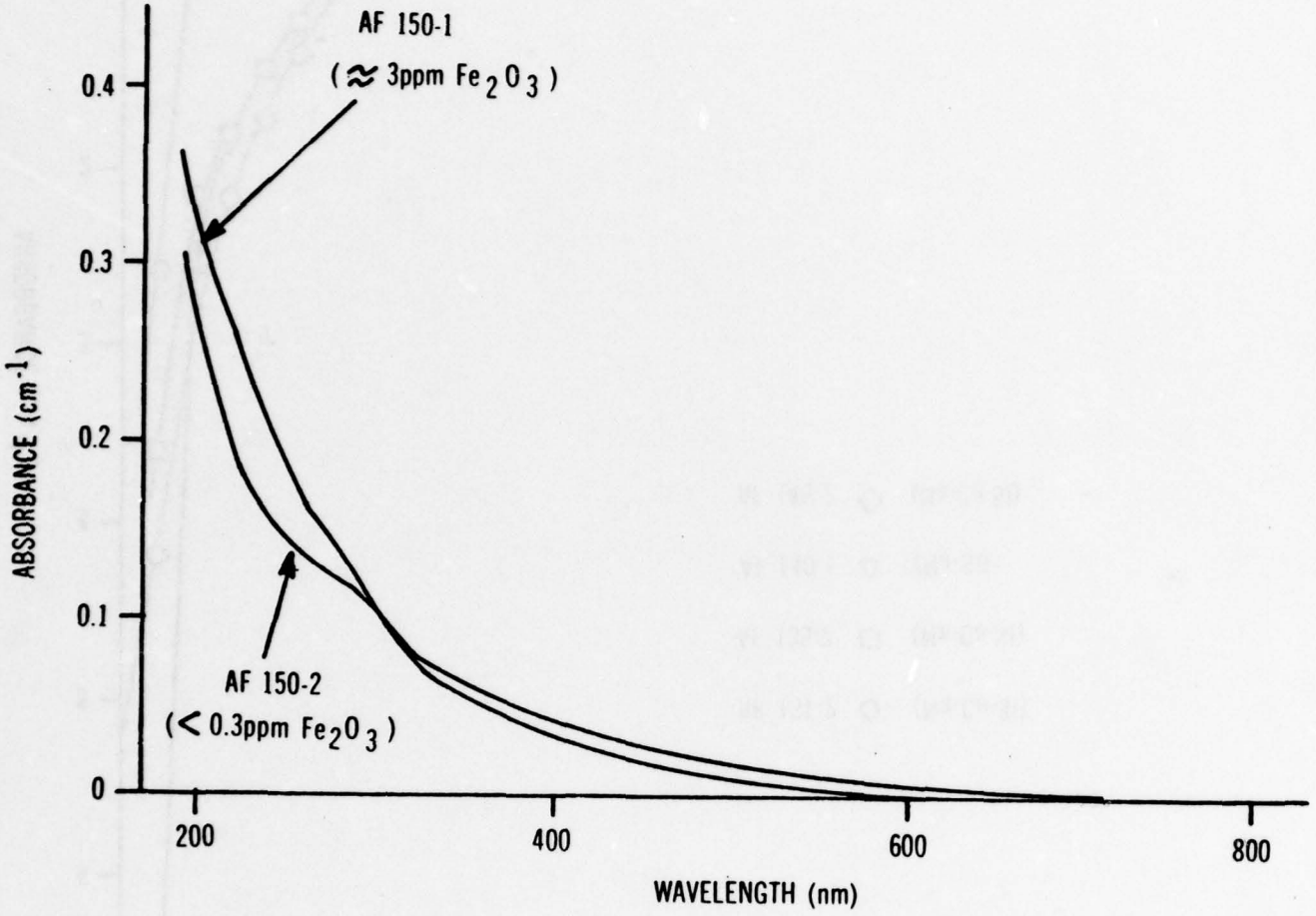

FIGURE 11. ABSORPTION SPECTRA OF "UNDOPED" Na_2O-CaO-B_2O_3 GLASSES CONTAINING DIFFERENT Fe_2O_3 LEVELS.

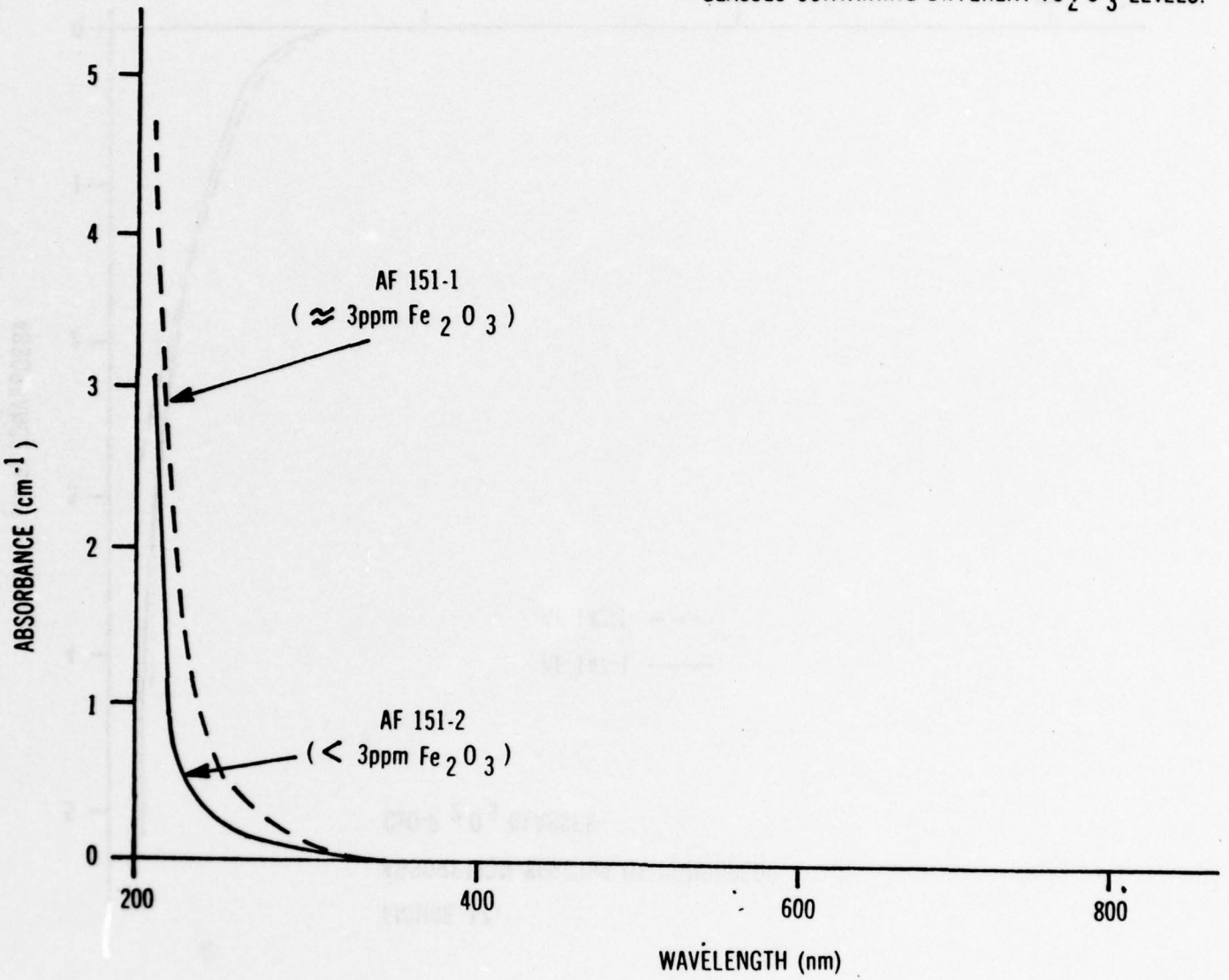

FIGURE 12.

ABSORPTION SPECTRA OF "UNDOPED"

$CaO\text{-}P_2O_5$ GLASSES.

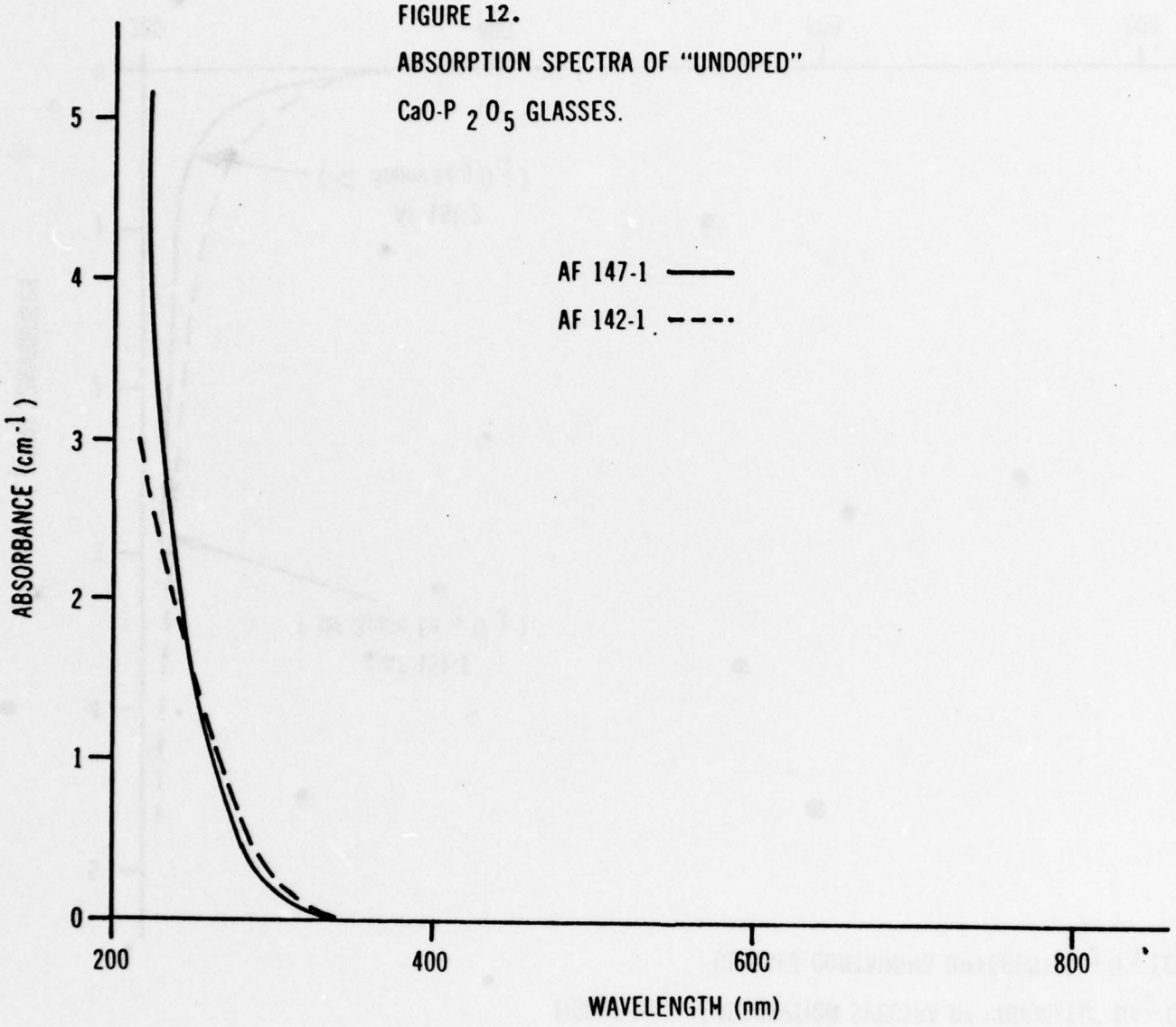

FIGURE 13. ABSORPTION AND EMISSION SPECTRA OF Cu + DOPED Na_2O-CaO-SiO_2 GLASSES. (REDUCING CONDITIONS)

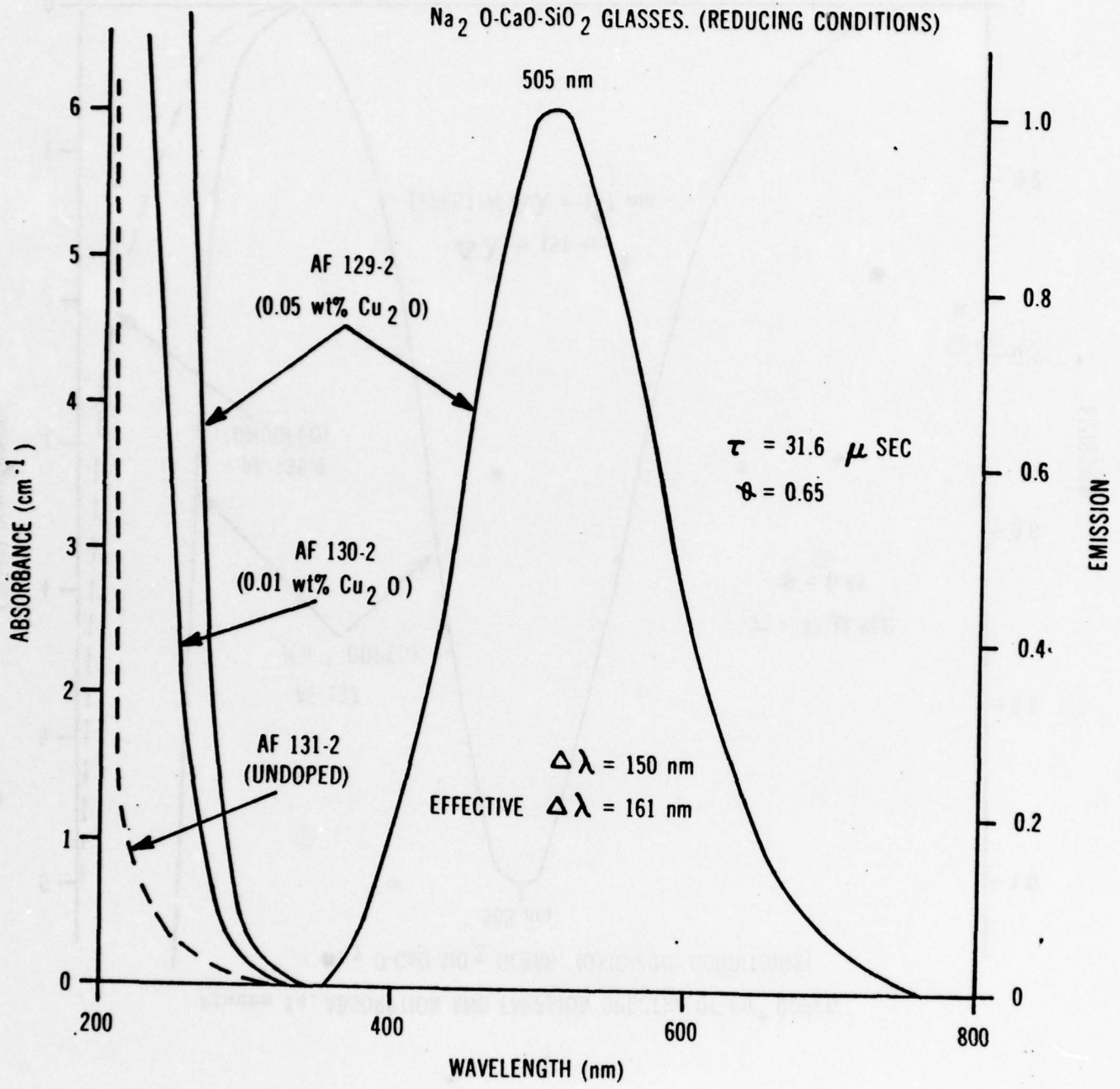

Figure 14. ABSORPTION AND EMISSION SPECTRA OF Cu^+ DOPED Na_2O-CaO-SiO_2 GLASS. (OXIDIZING CONDITIONS)

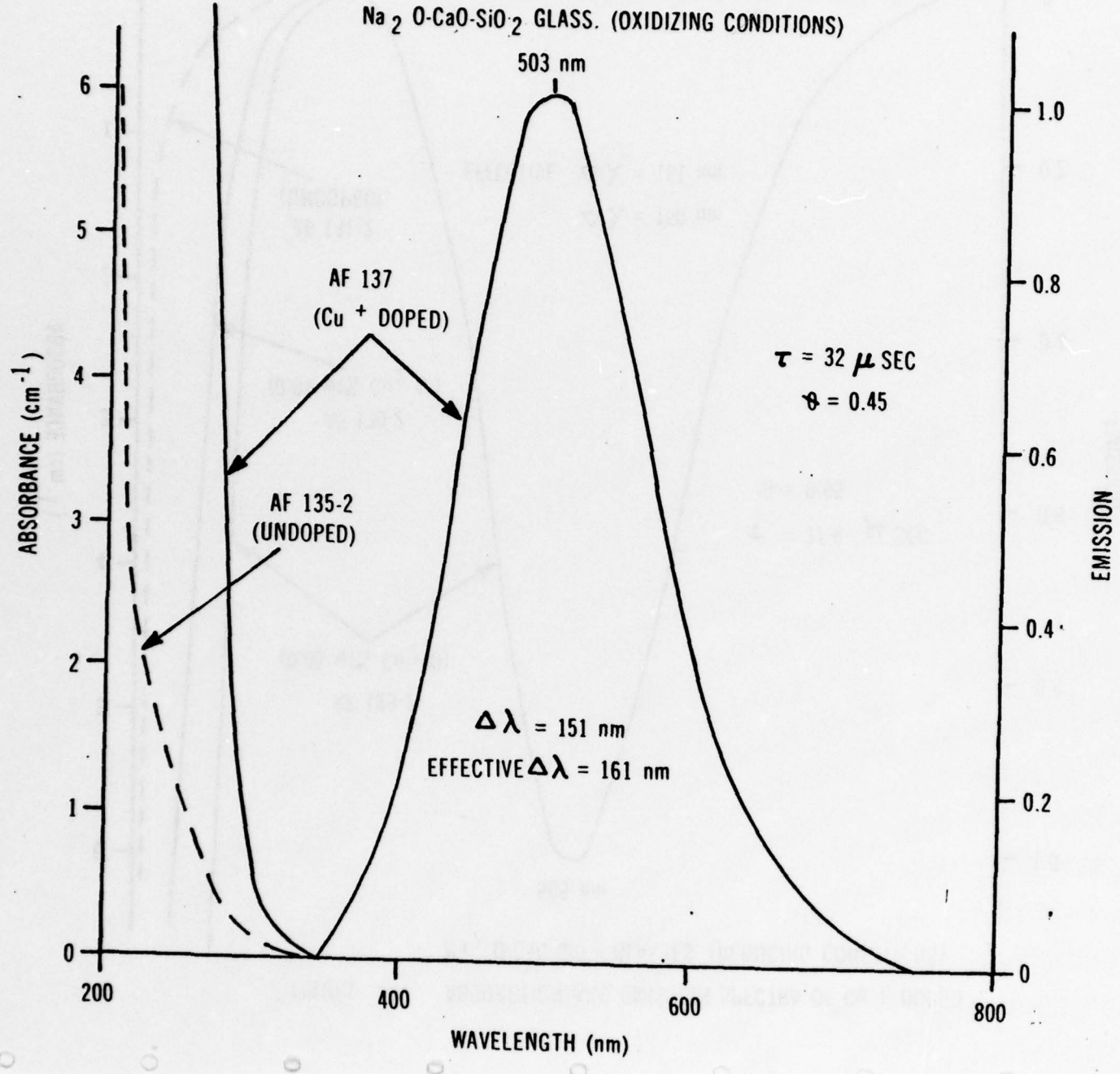

FIGURE 15. ABSORPTION AND EMISSION SPECTRA OF Cu^{+} + Sn^{2+} DOPED Na_2O-CaO-Sio_2 GLASS.

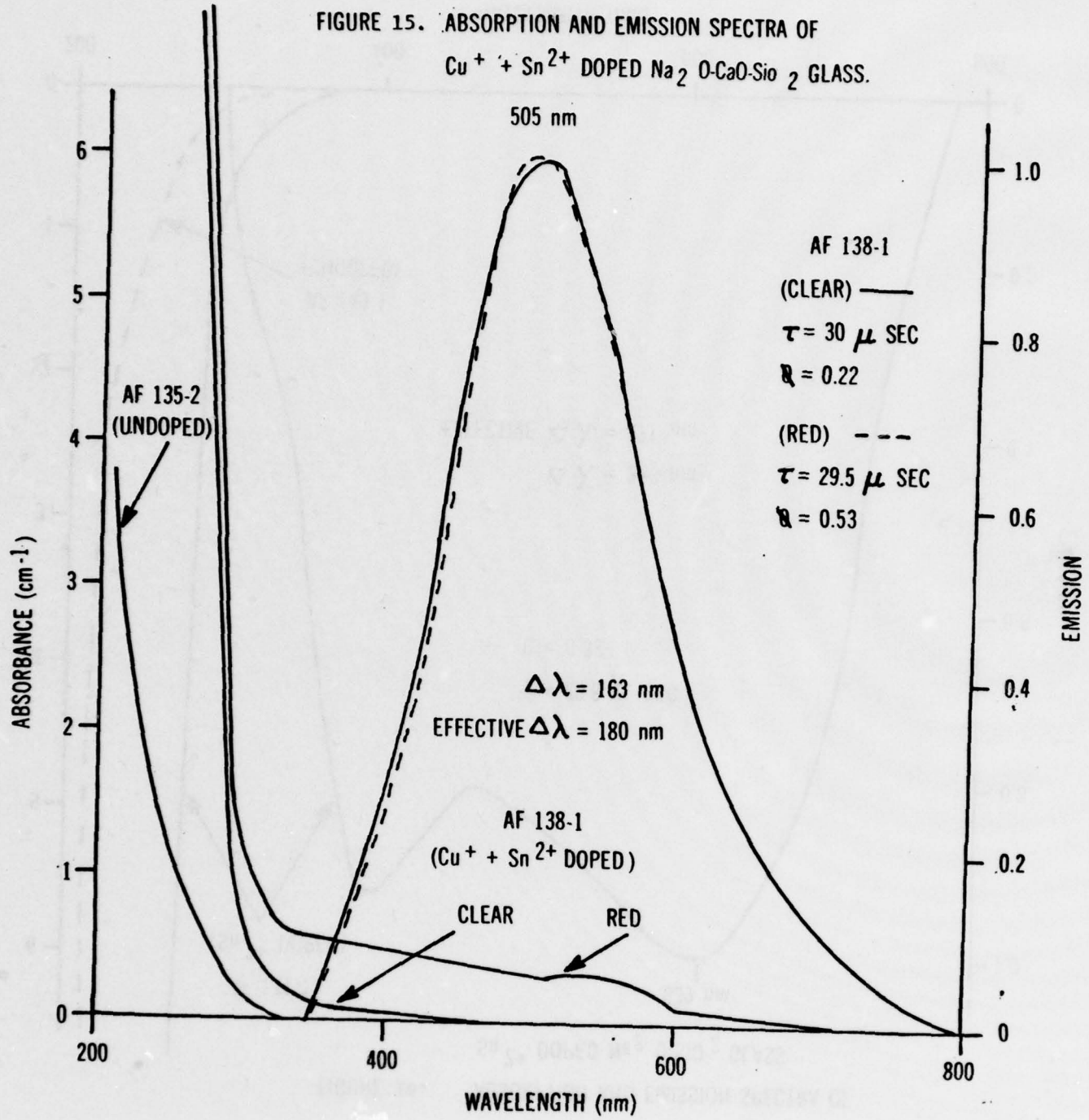

FIGURE 16. ABSORPTION AND EMISSION SPECTRA OF Sn^{2+} DOPED Na_2O-SiO_2 GLASS.

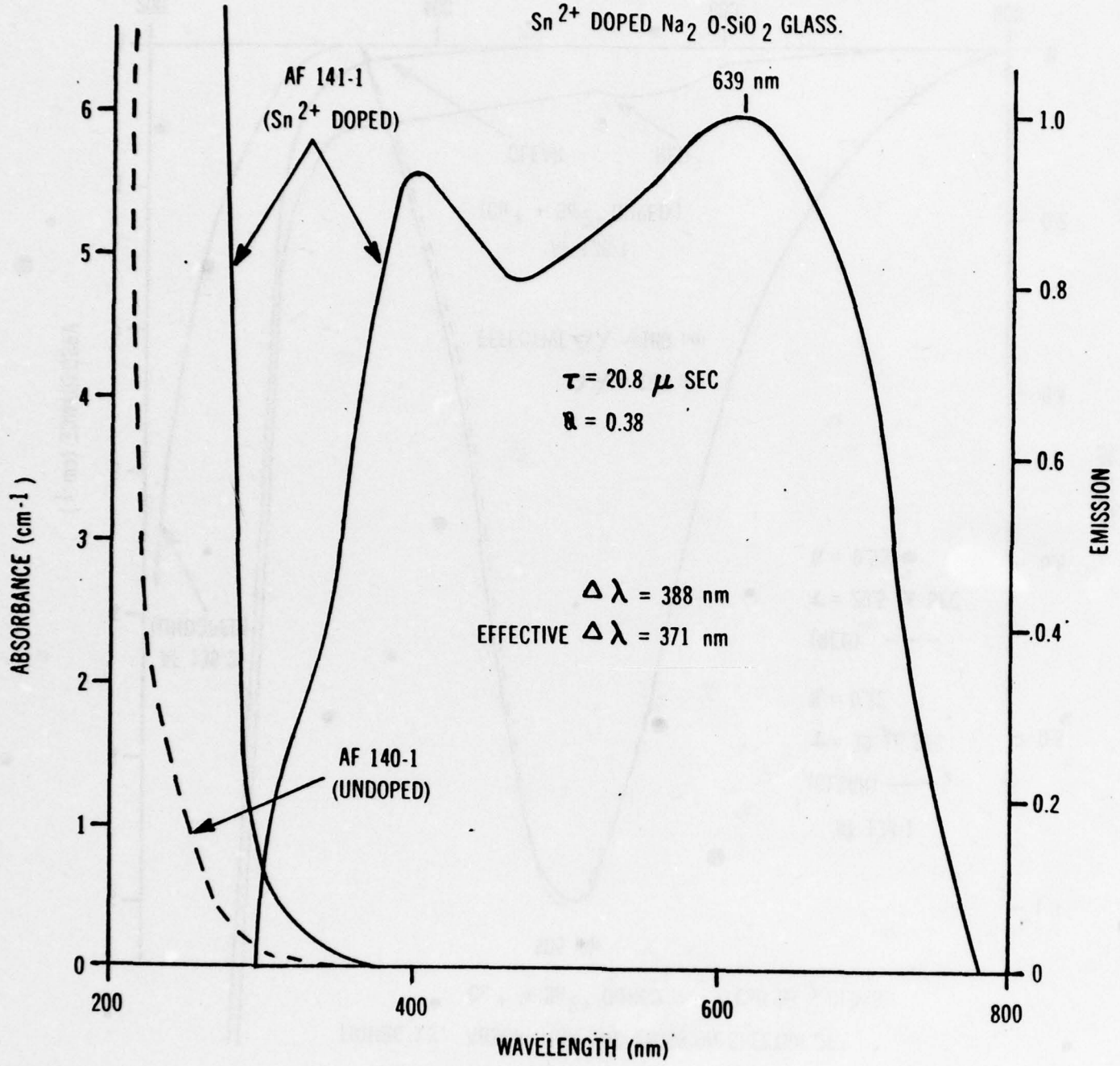

FIGURE 17. ABSORPTION AND EMISSION SPECTRA OF Sn^{2+} DOPED Na_2O-CaO-SiO_2 GLASS.

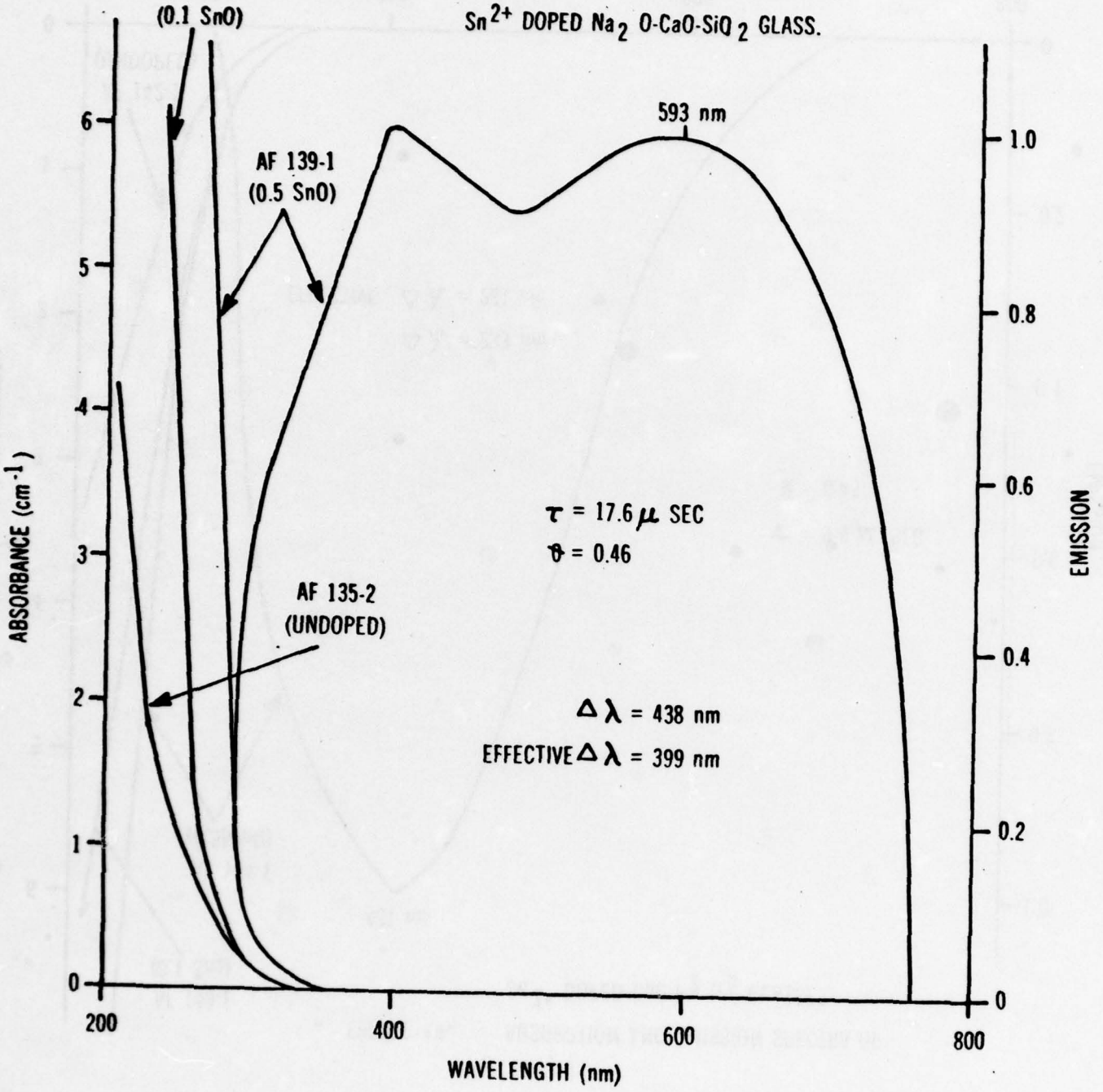

FIGURE 18. ABSORPTION AND EMISSION SPECTRA OF Sn^{2+} DOPED $CaO-P_2O_5$ GLASSES.

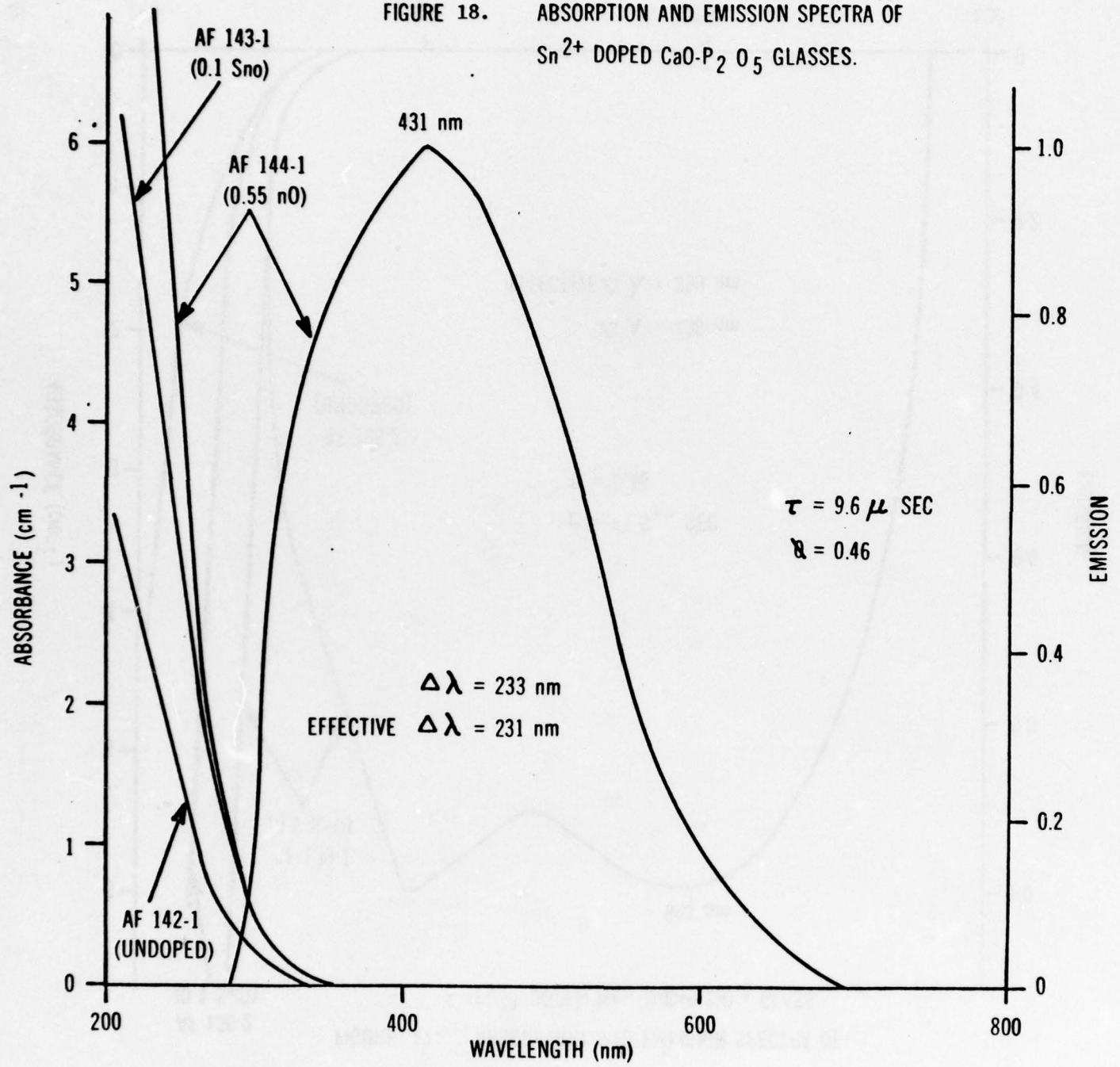

FIGURE 19. ABSORPTION AND EMISSION SPECTRA OF Sn^{2+} DOPED $CaO\text{-}P_2O_5$ GLASS.

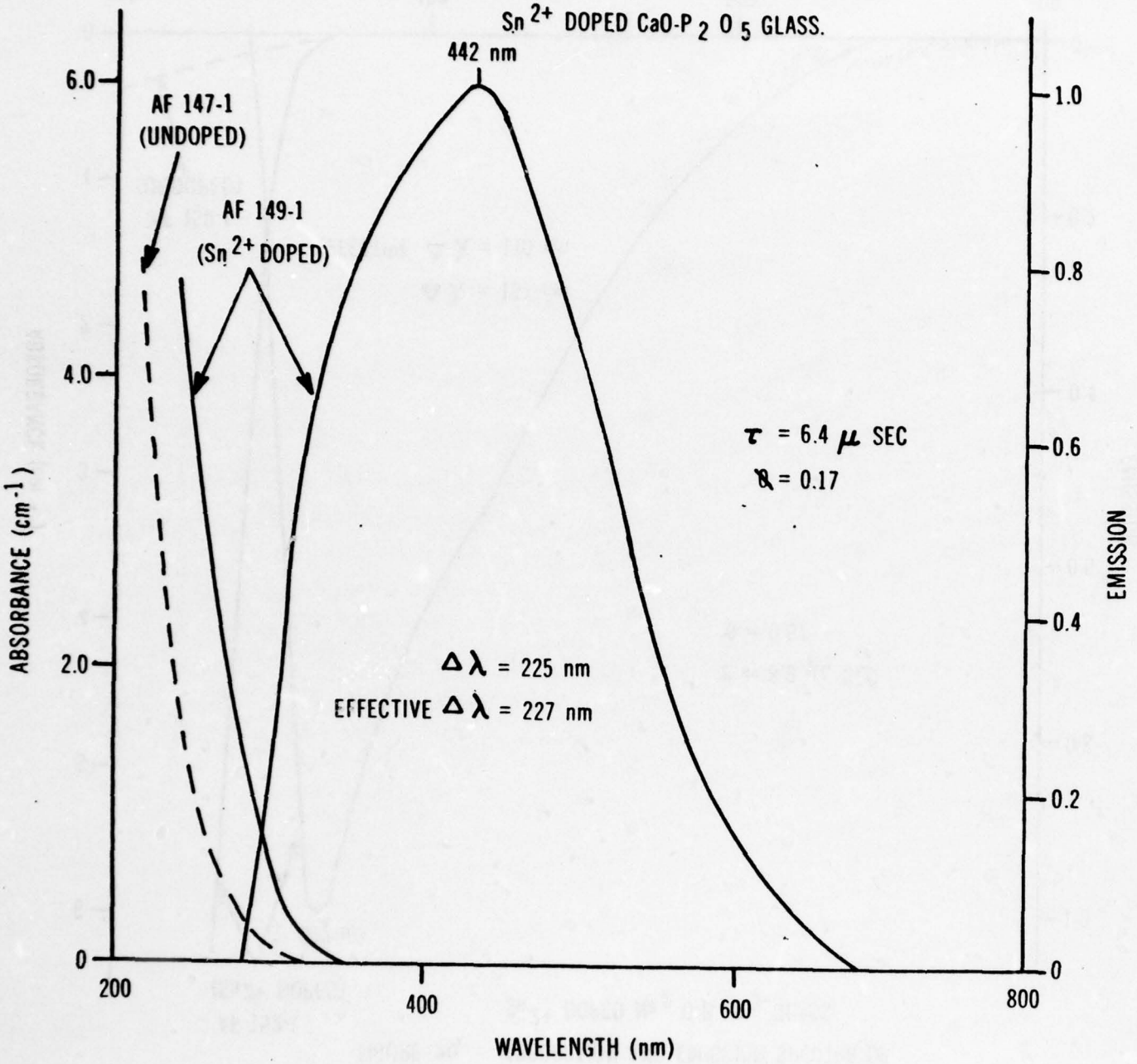

FIGURE 20. ABSORPTION AND EMISSION SPECTRA OF Sn^{2+} DOPED Na_2O-B_2O_3 GLASS.

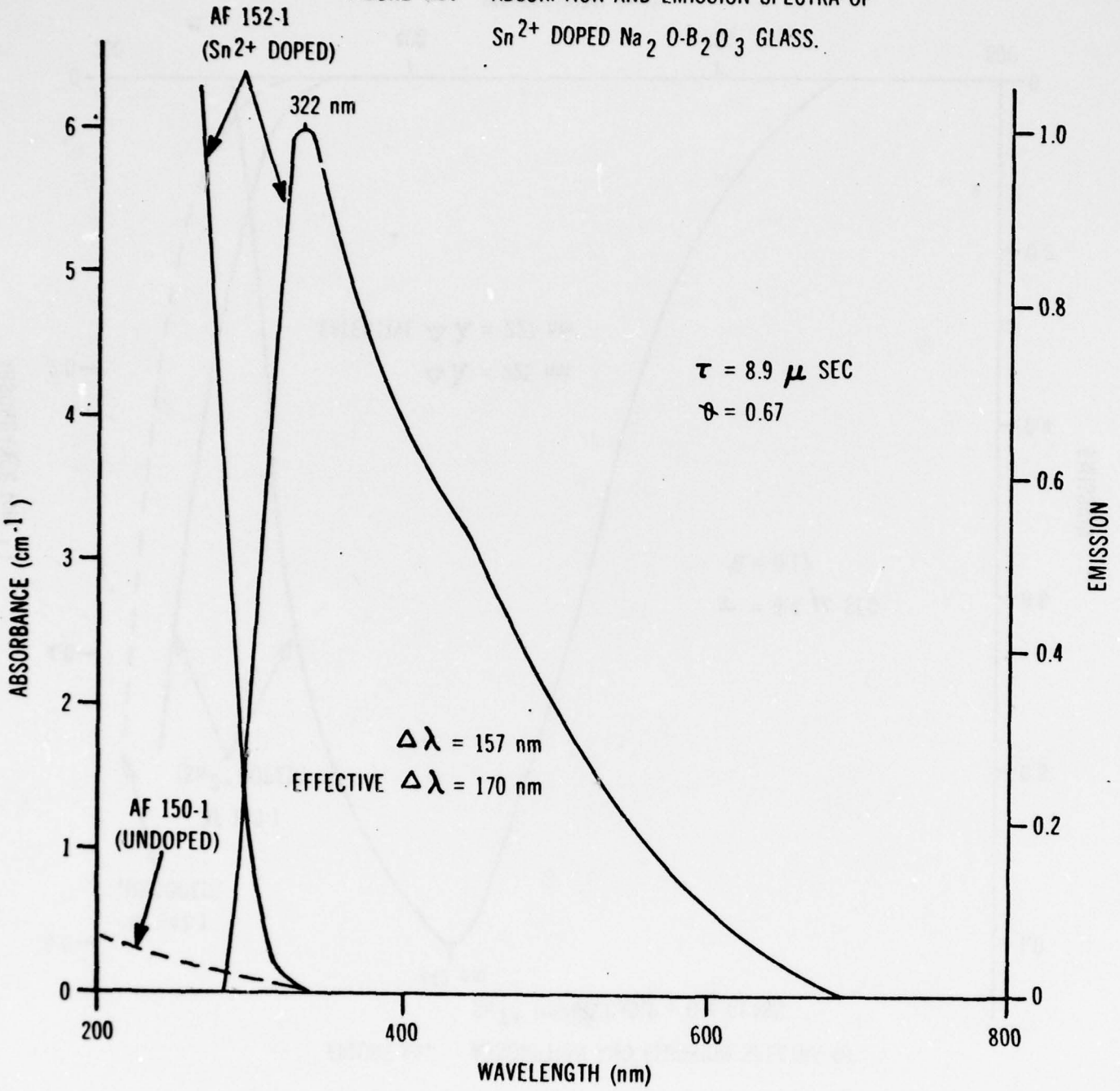

FIGURE 21. ABSORPTION AND EMISSION SPECTRA OF Sn^{2+} DOPED Na_2O-CaO-B_2O_3 GLASS.

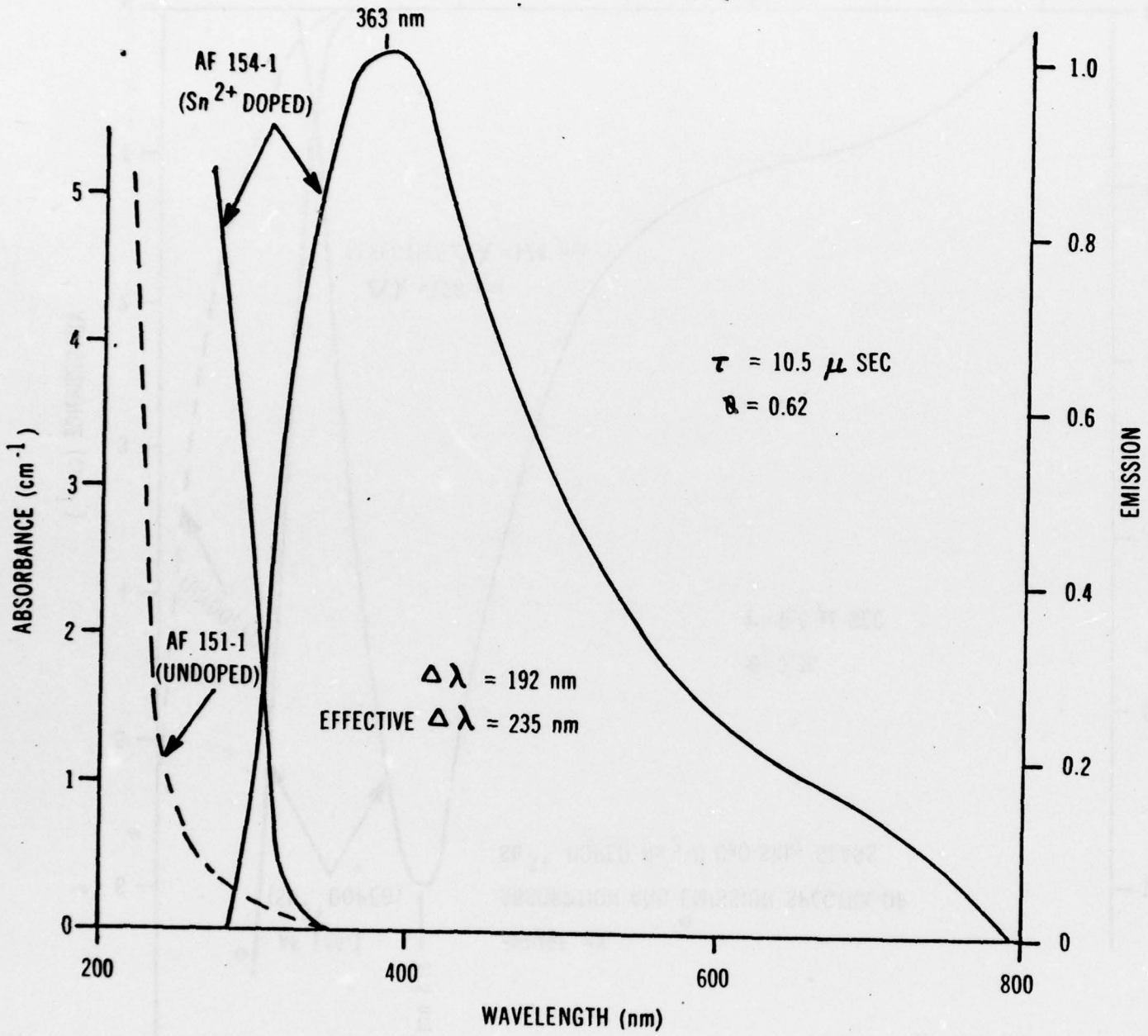

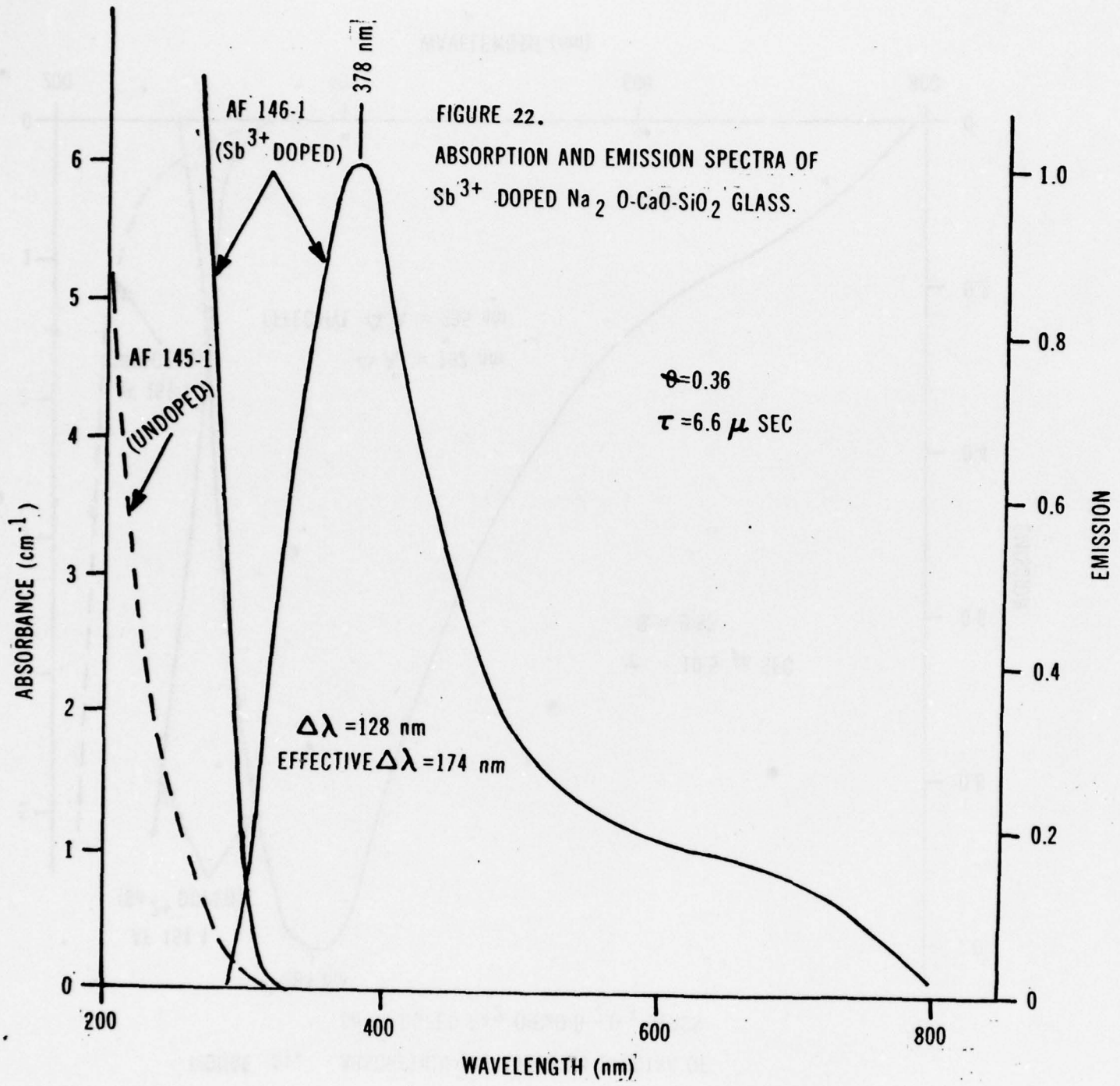

FIGURE 22.
ABSORPTION AND EMISSION SPECTRA OF
Sb^{3+} DOPED Na_2O-CaO-SiO_2 GLASS.

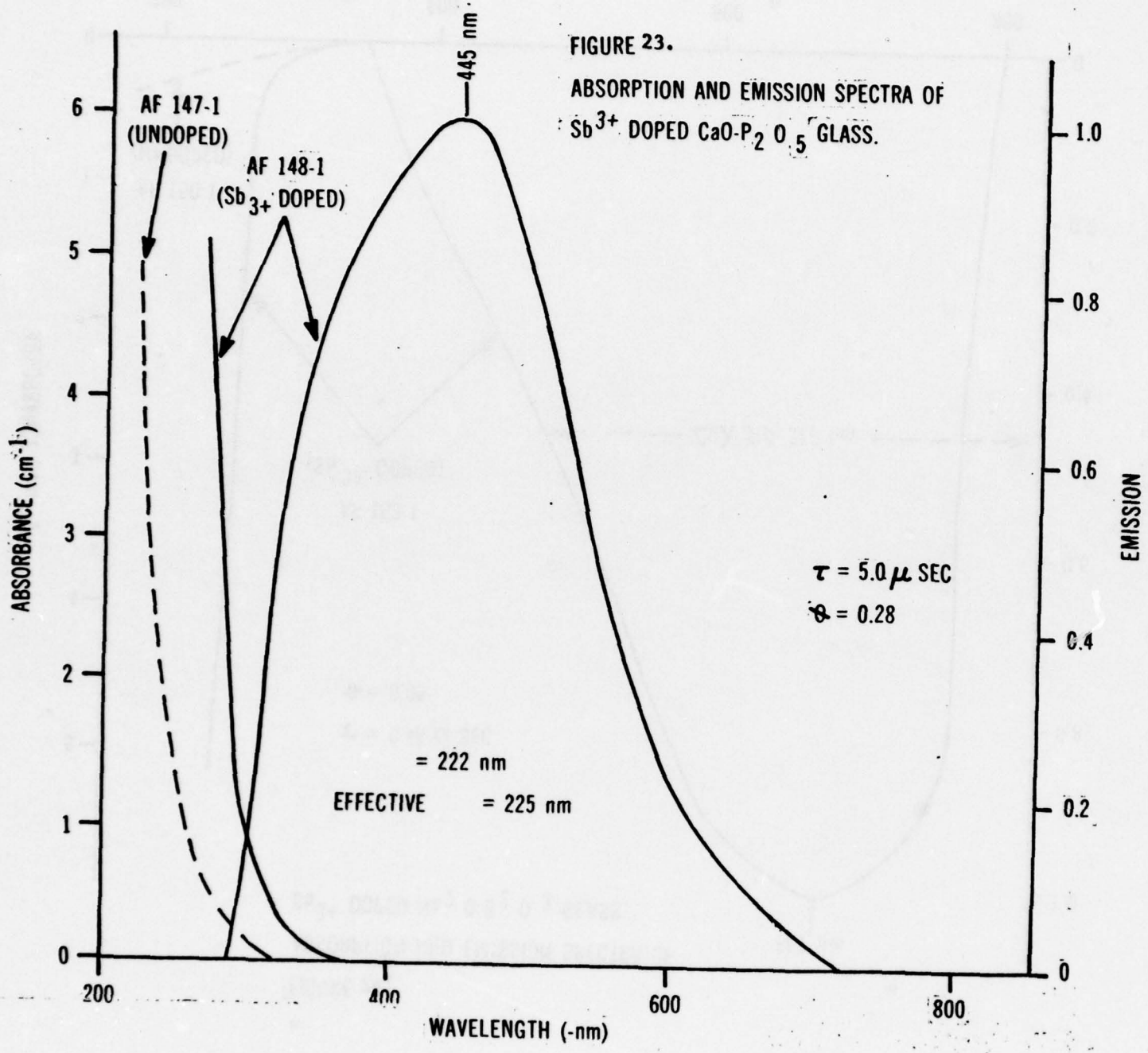

FIGURE 23.

ABSORPTION AND EMISSION SPECTRA OF Sb^{3+} DOPED $CaO-P_2O_5$ GLASS.

FIGURE 24.

ABSORPTION AND EMISSION SPECTRA OF Sb^{3+} DOPED Na_2O-B_2O_3 GLASS.

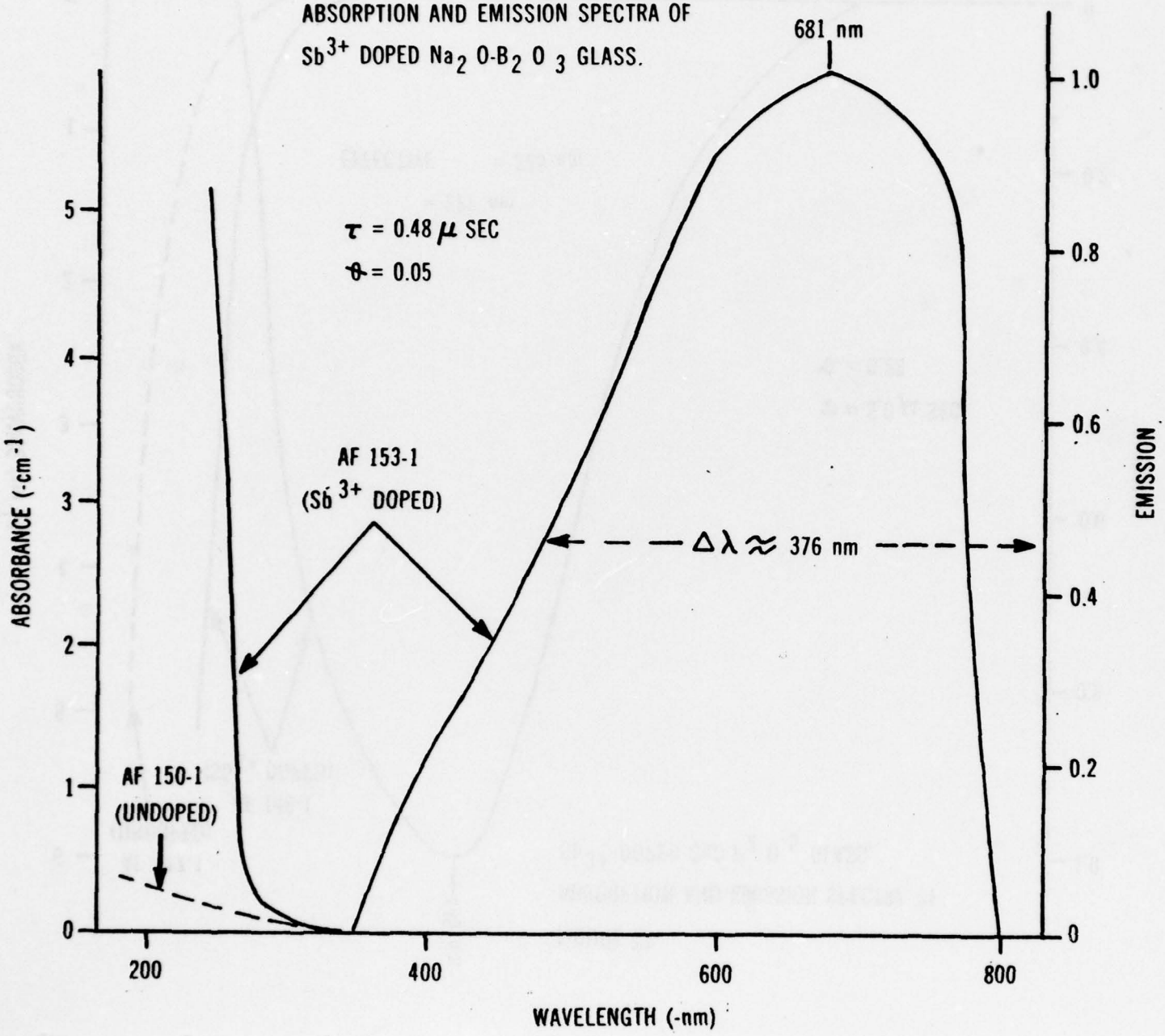

FIGURE 25. ABSORPTION AND EMISSION SPECTRA OF Sb^{3+} DOPED Na_2O-CaO-B_2O_3 GLASS.

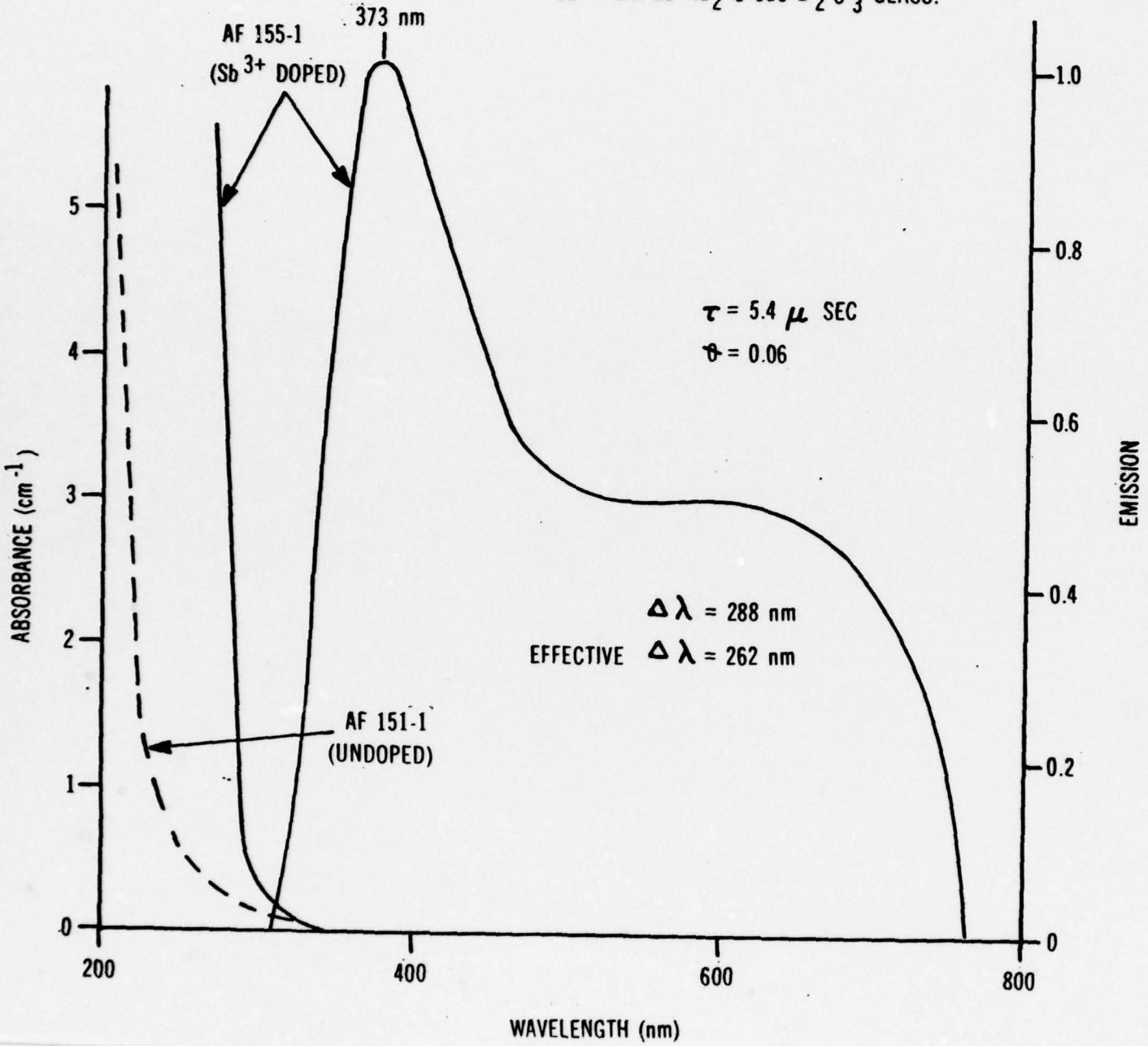

Appendix I.

Observed Pumped Absorptions vs. Time Data

Cu^{+} Doped Na_2O–CaO–SiO_2 (Reduced)

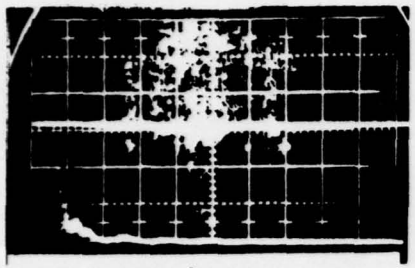

AF129 1 μsec/div λ = 6328

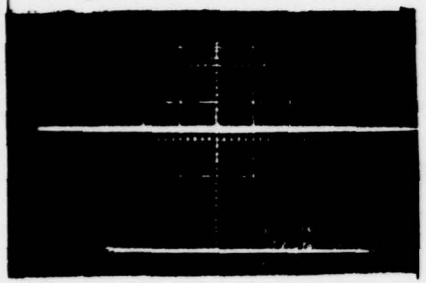

AF129 1 μsec/div λ = 5017Å

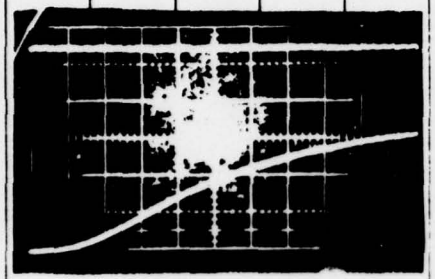

AF129 10 msec/div λ = 5017Å

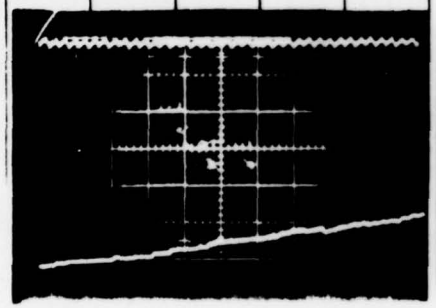

AF129 10 msec/div λ = 4545Å

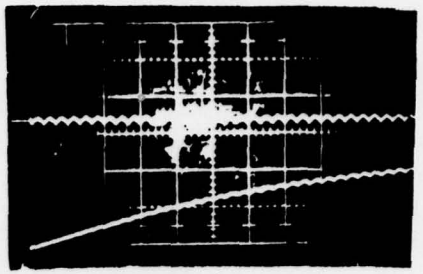

AF129 50 msec/div λ = 6328

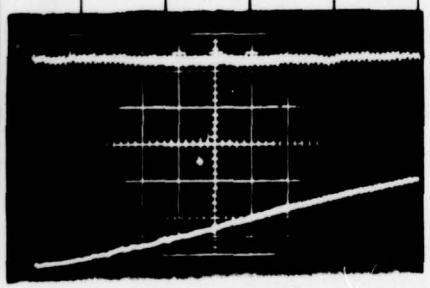

AF129 20 msec/div λ = 4545Å

Cu^{+} Doped Na_2O-CaO-SiO_2 (Oxidized Blue)

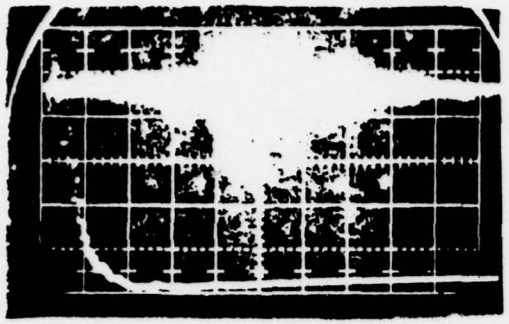

AF137 1 sec/div λ = 6328

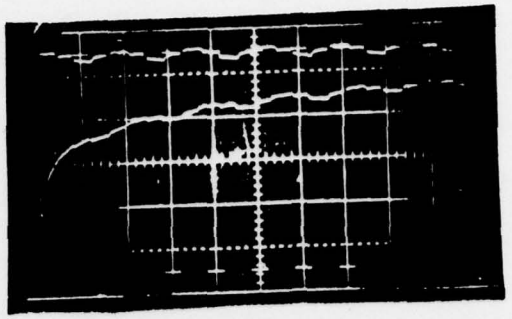

AF137 10 m sec/div λ = 6328

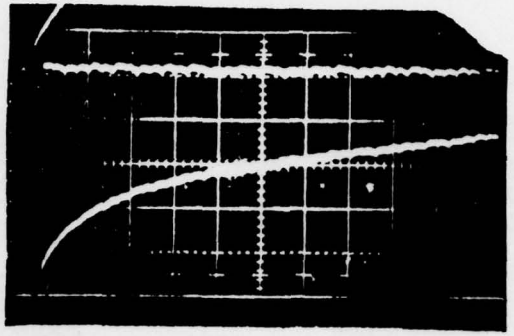

AF137 10 m sec/div λ = 5017

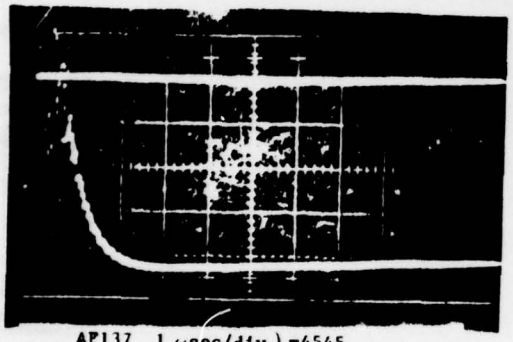

AF137 1 μsec/div λ =4545

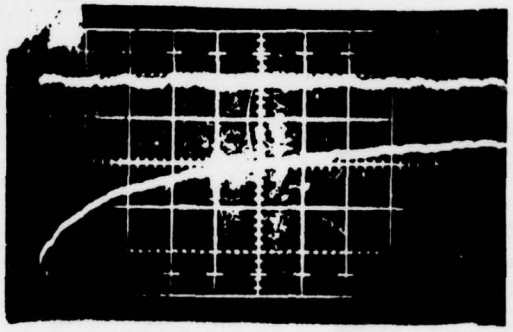

AF137 10 m sec/div λ = 4545

Cu^{+} Doped Na_2O–CaO–SiO_2(Reduced)

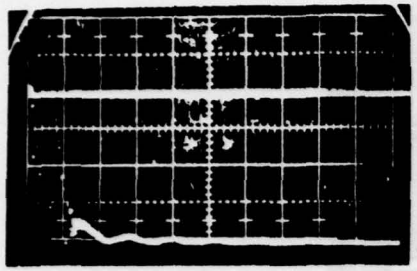

AF130 1 μsec/div λ = 6328Å

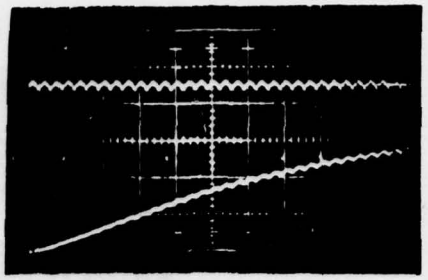

AF130 50 μsec/div λ = 6328Å

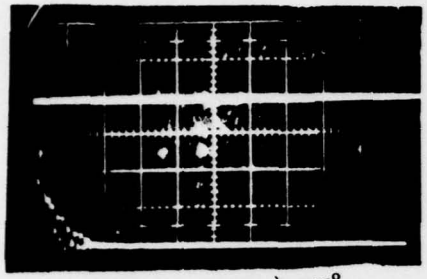

AF130 10 μsec/div λ=5017Å

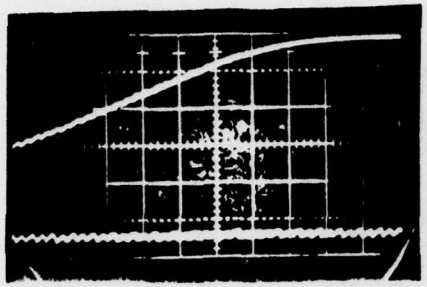

AF130 1 μsec/div λ= 5017Å

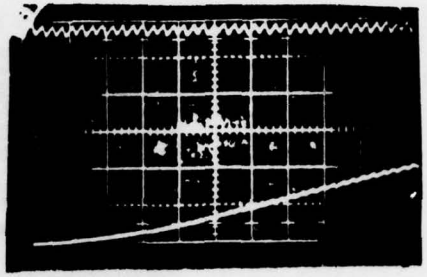

AF130 10 μ sec/div λ= 4545Å

Eu^{2+} IN VYCOR

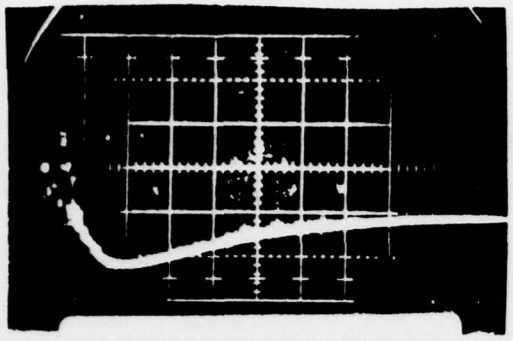

Eu^{2+} in Vycor 1 μsec/div
λ= 5017Å

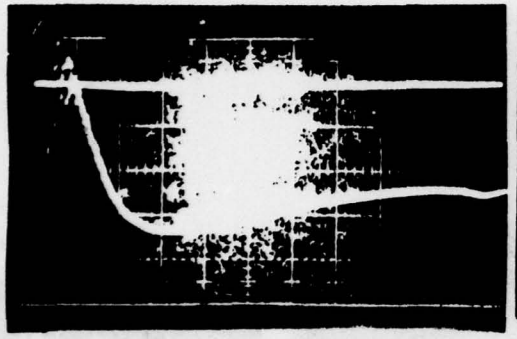

Eu^{2+} in Vycor 1 μsec/div
λ= 4545

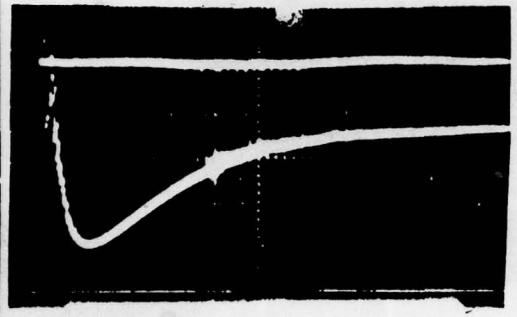

Eu^{2+} in Vycor 2 μsec/div
= 4545

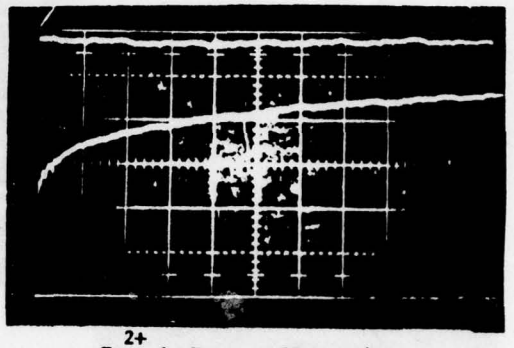

Eu^{2+} in Vycor 10 μsec/div
λ= 4545

$Sn^{+} + Cu^{+}$ Doped Na_2O-CaO-SiO_2 (Red)

AF138 1 μsec/div λ = 6328

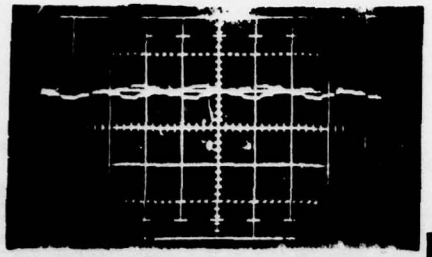

AF138 10 msec/div λ = 6328

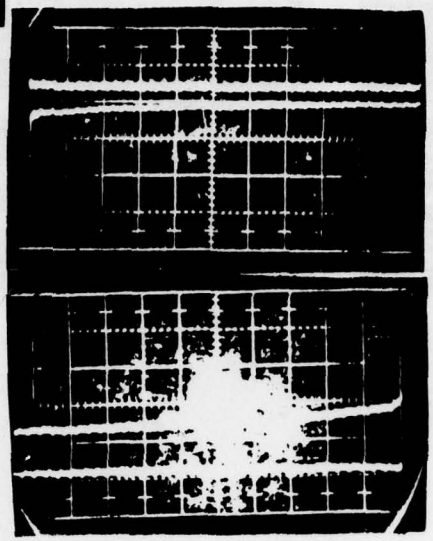

AF138 50 msec/div λ = 5017

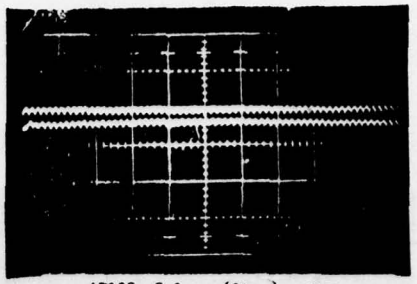

AF138 0.1 sec/div λ = 6328

ABSORBED TO STRONG TO GET MEASUREMENT

Sn^{2+} Doped Na_2O–CaO–SiO_2

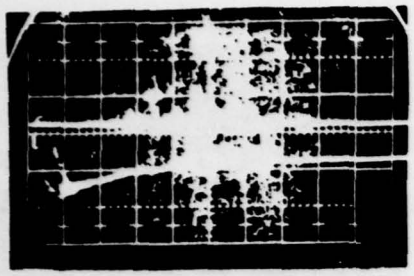

AF136 1 sec/div - 6328

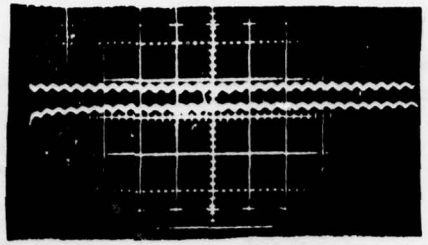

AF136 50 msec/div λ = 6328

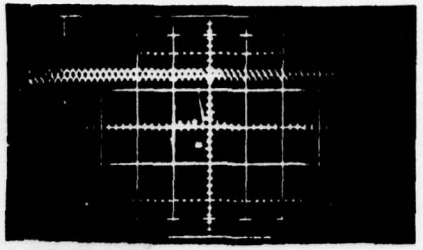

AF136 0.1 sec/div λ = 6328Å

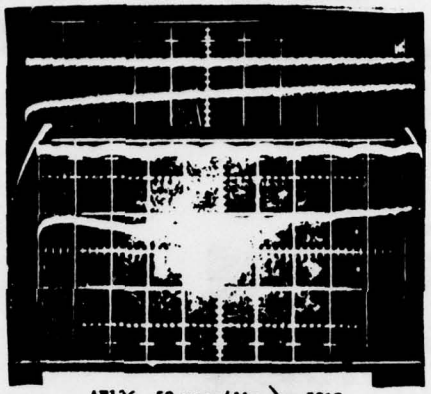

AF136 50 msec/div λ = 5017

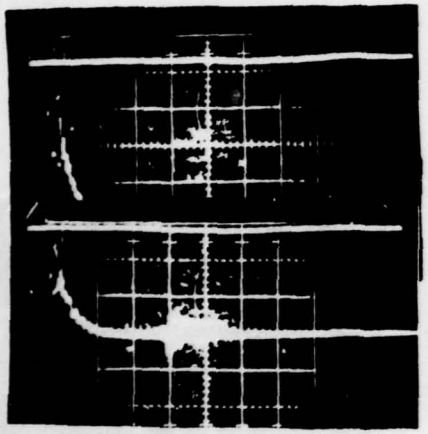

AF136 1 msec/div λ = 4545 (1/4")

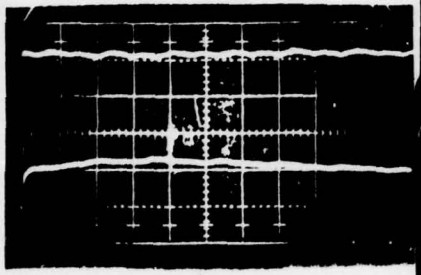

AF136 10 msec/div λ = 4545

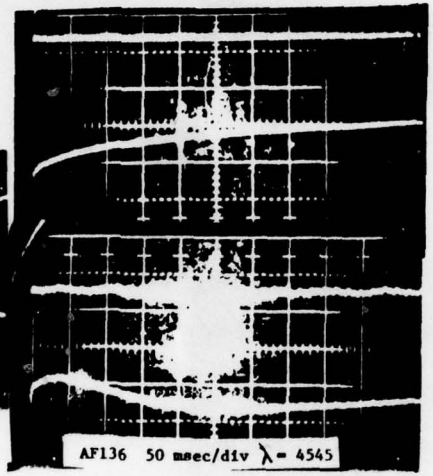

AF136 50 msec/div λ = 4545

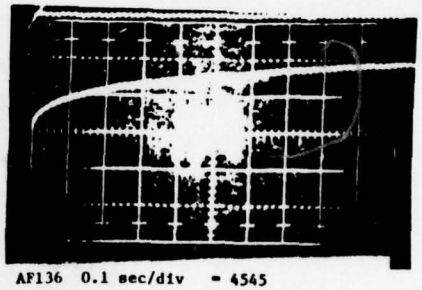

AF136 0.1 sec/div = 4545

Sn^{2+} Doped Na_2O–CaO–SiO_2

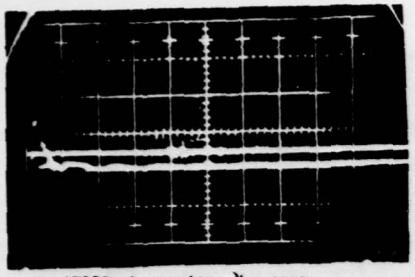

AF139 1 μsec/div λ = 6328

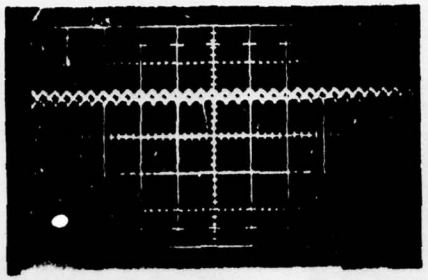

AF139 50 msec/div λ = 6328

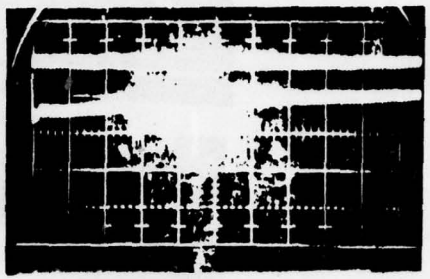

AF139 50 msec/div λ = 5017

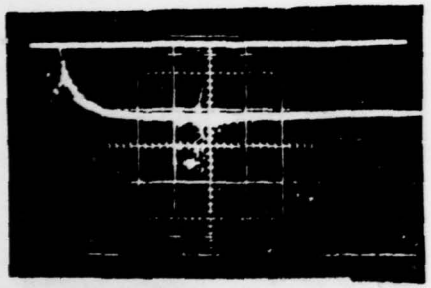

AF139 1 μsec/div λ = 4545

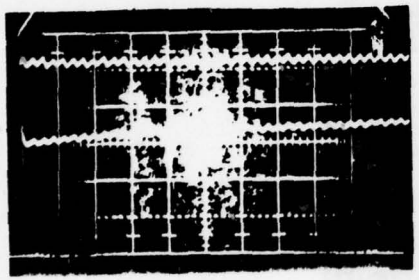

AF139 10 msec/div λ = 4545

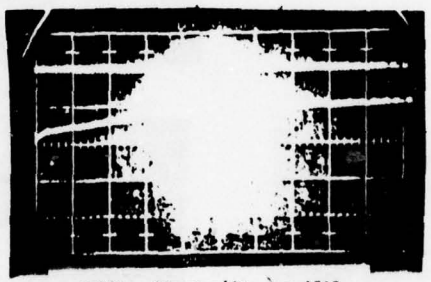

AF139 50 msec/div λ = 4545

Sn^{2+} Doped $CaO-P_2O_5$

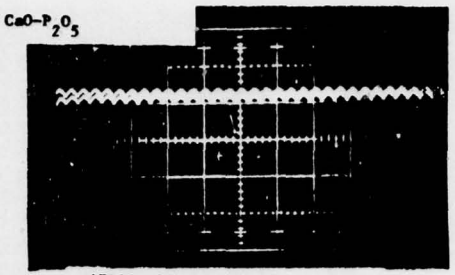

AF149 50 msec/div λ= 6328

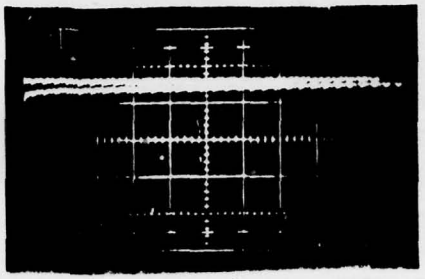

AF149 50 msec/div λ= 5017

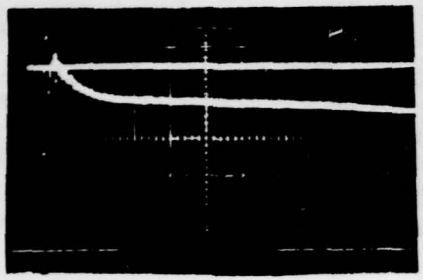

AF149 1 msec/div λ= 4545

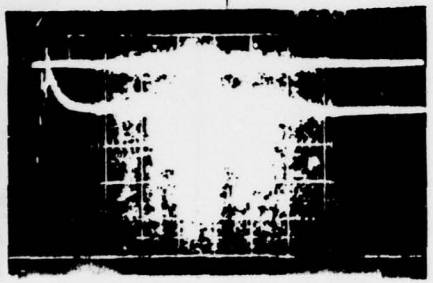

AF149 2 μsec/div λ= 4545

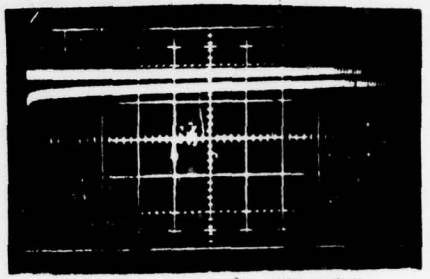

AF149 0.2 sec/div λ= 4545 (1/4")

Sn^{2+} Doped Na_2O–CaO–B_2O_3

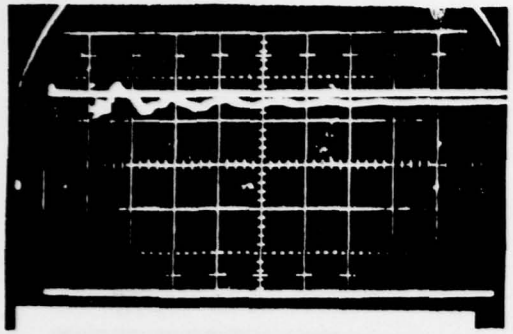

AF154 1 μsec/div λ= 6328

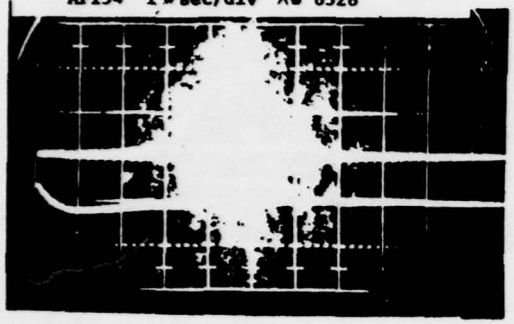

AF154 1 μsec/div λ= 5017

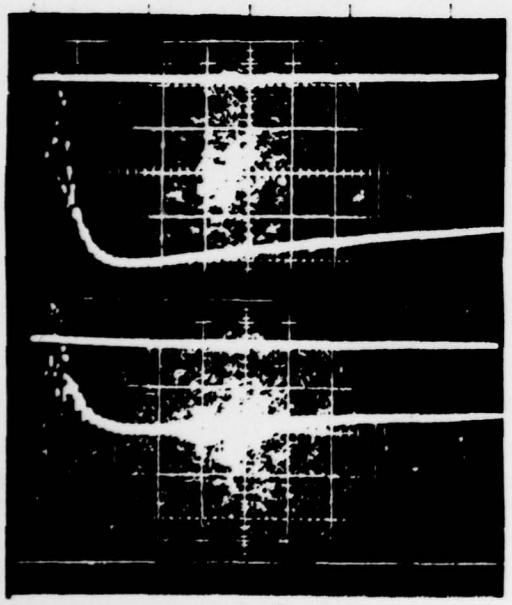

AF154 1 μsec/div λ= 4545 (1/4")

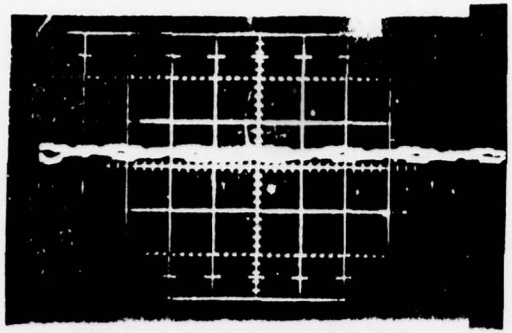

AF154 10 msec/div λ = 6328

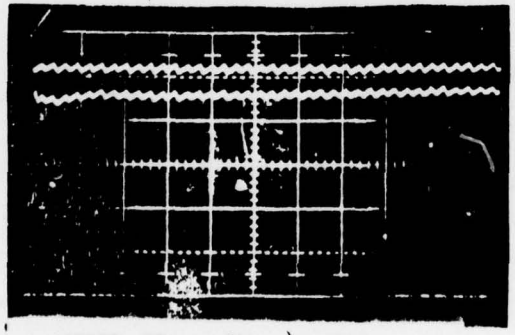

AF154 10 msec/div λ= 4545

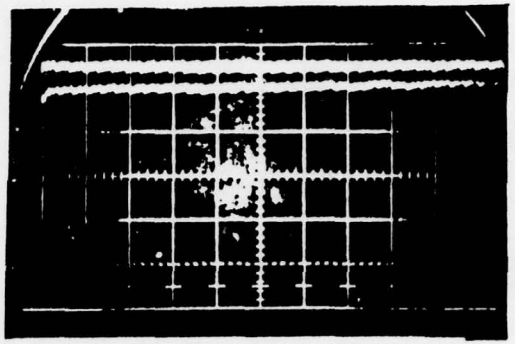

AF154 50 msec/div λ= 5017

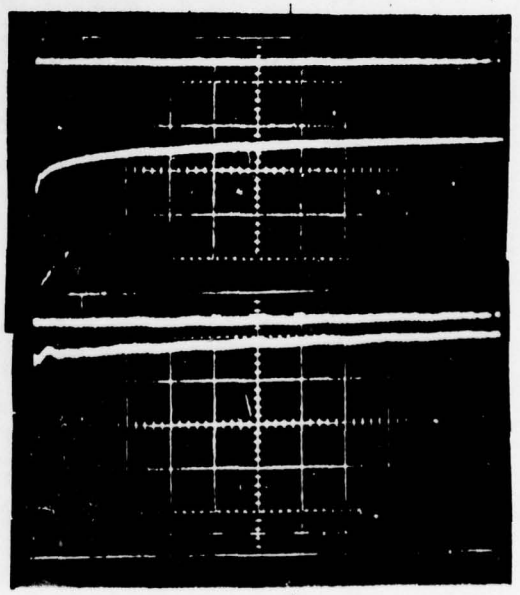

AF154 50 msec/div λ = 4545

Sb^{3+} Na_2O–CaO–SiO_2

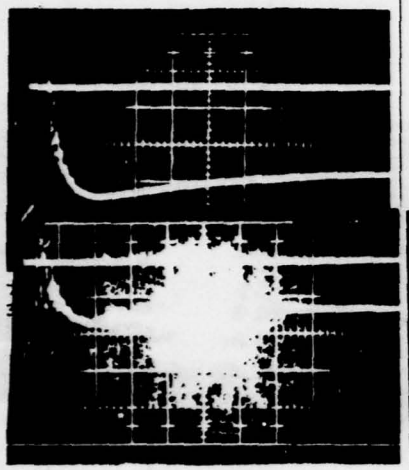

AF146 1 msec/div λ = 4545

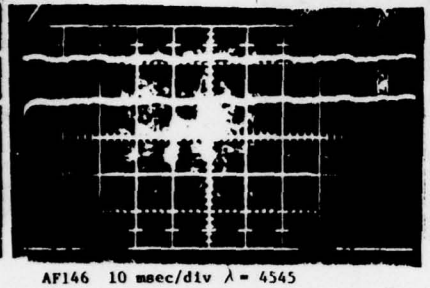

AF146 10 msec/div λ = 4545

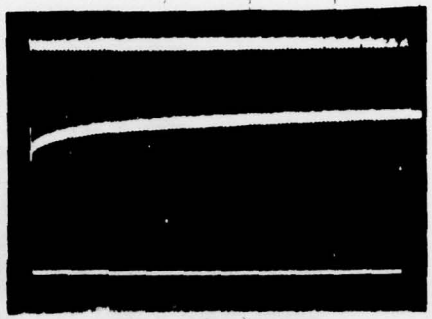

AF146 50 msec/div λ = 4545 (3 mm)

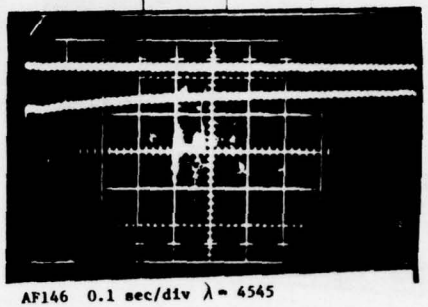

AF146 0.1 sec/div λ = 4545

Sb^{3+} Doped C50-P_2O_5

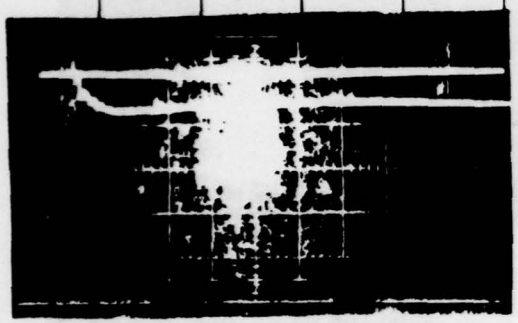

AF148 1 μsec/div λ= 4545

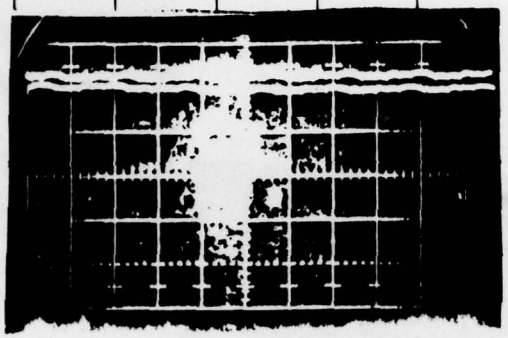

AF148 10 msec/div λ= 4545

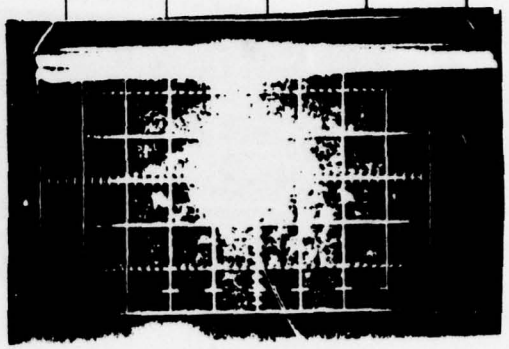

AF148 0.2 sec/div λ= 4545

Sb^{3+} Doped Na_2O–CaO–B_2O_3

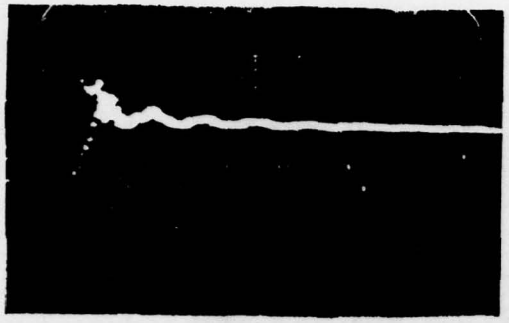

AF155 1 μsec/div λ = 6328

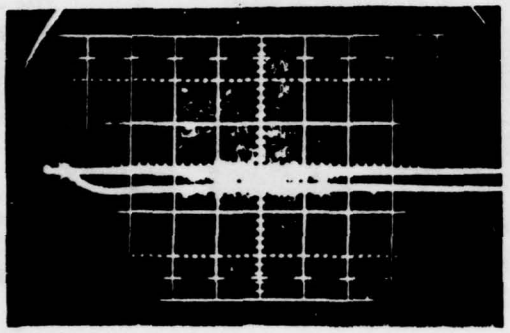

AF155 1 μsec/div λ = 5017

Undoped Na_2O–CaO–SiO_2 (Reduced)

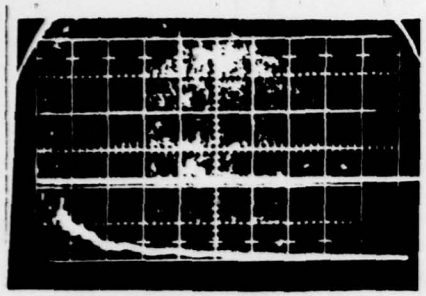

AF131-1 1 μsec/div λ = 6328

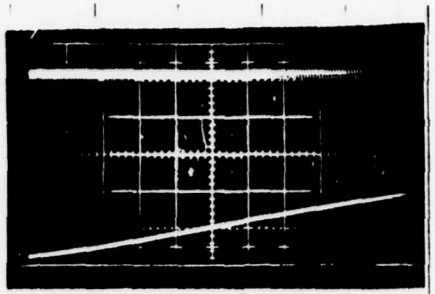

AF131-2 0.2 sec/div λ = 6328

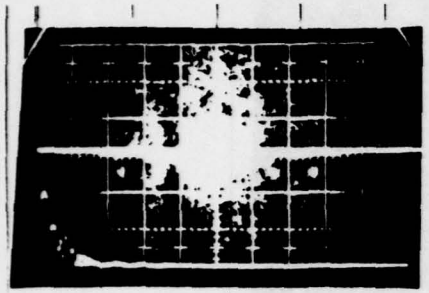

AF131-1 1 msec/div λ = 5017

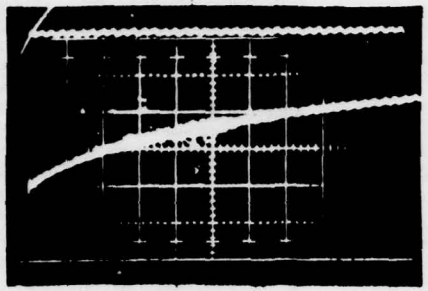

AF131-2 10 msec/div λ = 5017 (reduced voltage)

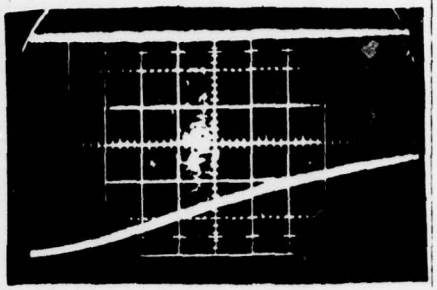

AF131-2 50 msec/div λ = 5017

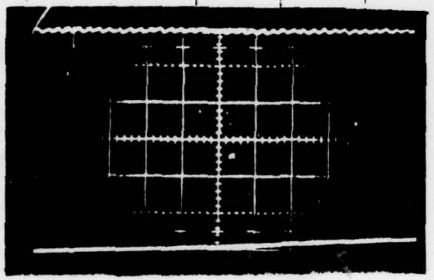

AF131-2 10 msec/div λ = 4545

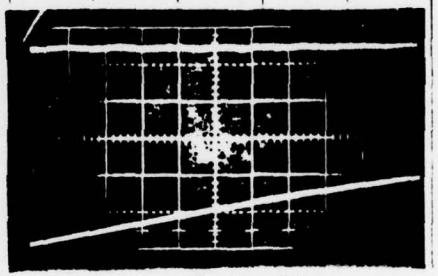

AF131-2 50 msec/div λ = 4545

Undoped Na_2O-CaO-SiO_2 (Oxidized)

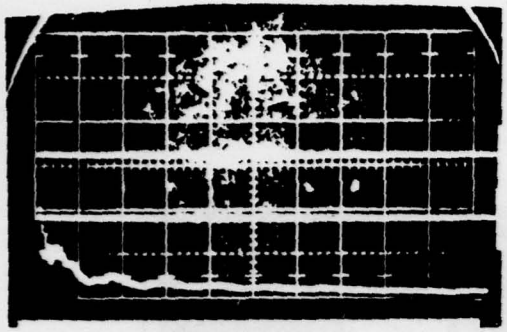

AF135-2 1 μsec/div λ = 6328

Before

After

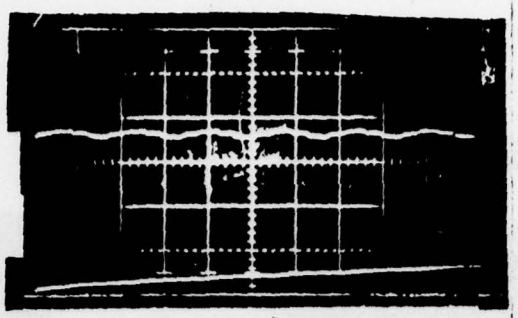

AF135-1 10 msec/div λ = 6328

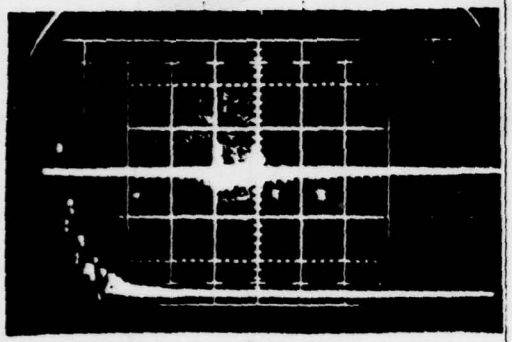

AF135-2 1 μsec/div λ = 5017

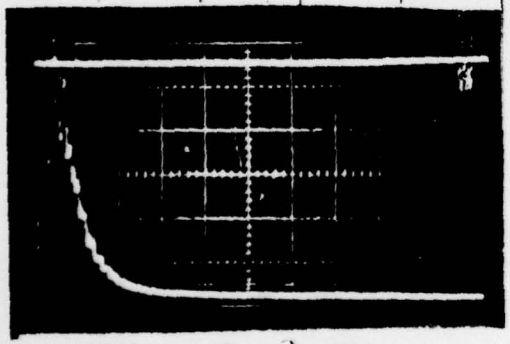

AF135-2 1 μsec/div. λ = 4545

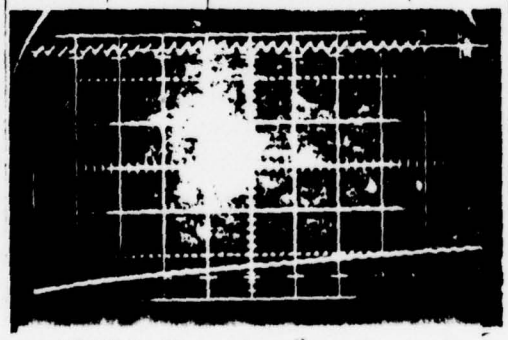

AF135-2 10 msec/div λ = 4545

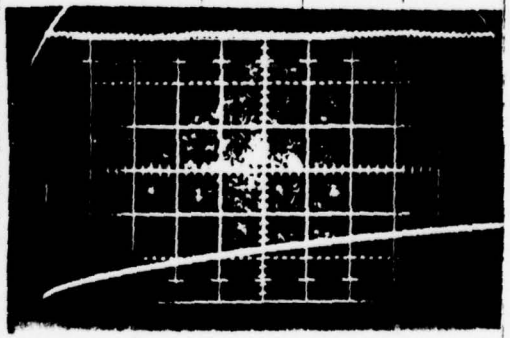

AF135-2 20 msec/div λ = 4545

Sn^{2+} Doped Na_2O–B_2O_3

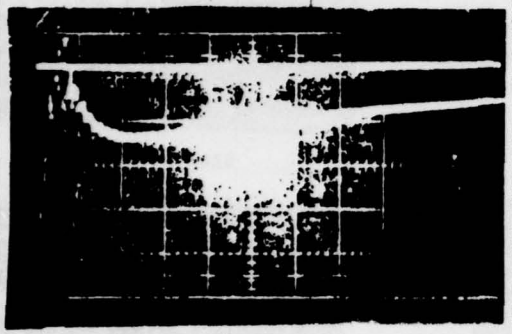

AF152 1 μsec/div λ=4545Å

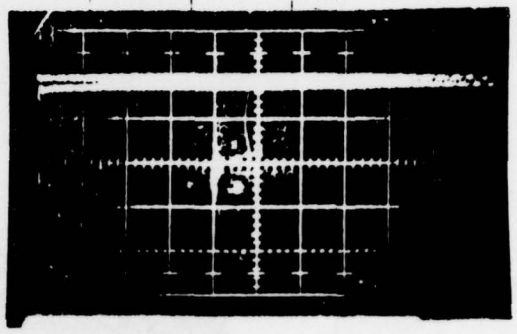

AF152 50 msec/div
λ=4545 (1/4")

Undoped Na_2O-CaO-SiO_2 (Oxidized)

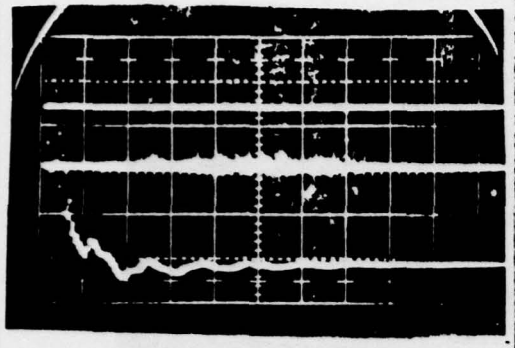

AF145-2 1 μsec/div λ = 6328

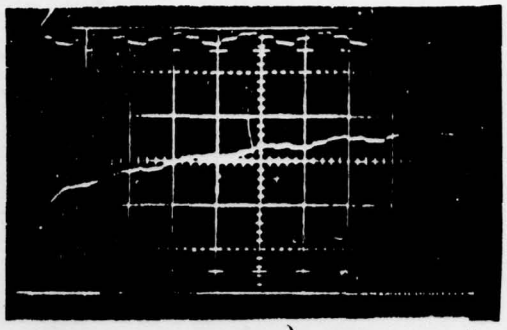

AF145-2 10 msec/div λ = 6328

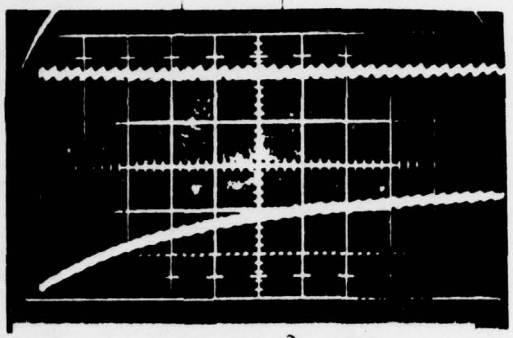

AF145-2 10 msec/div λ = 5017

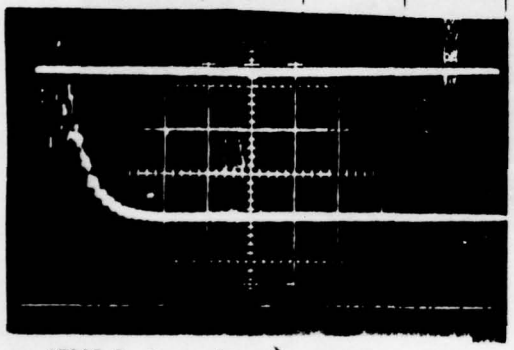

AF145-2 1 μsec/div λ = 4545

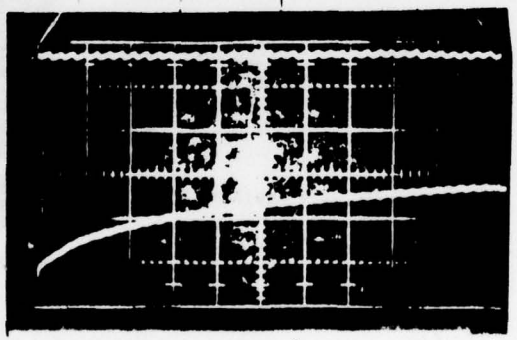

AF145-2 10 msec/div λ = 4545

Undoped $CaO-P_2O_5$

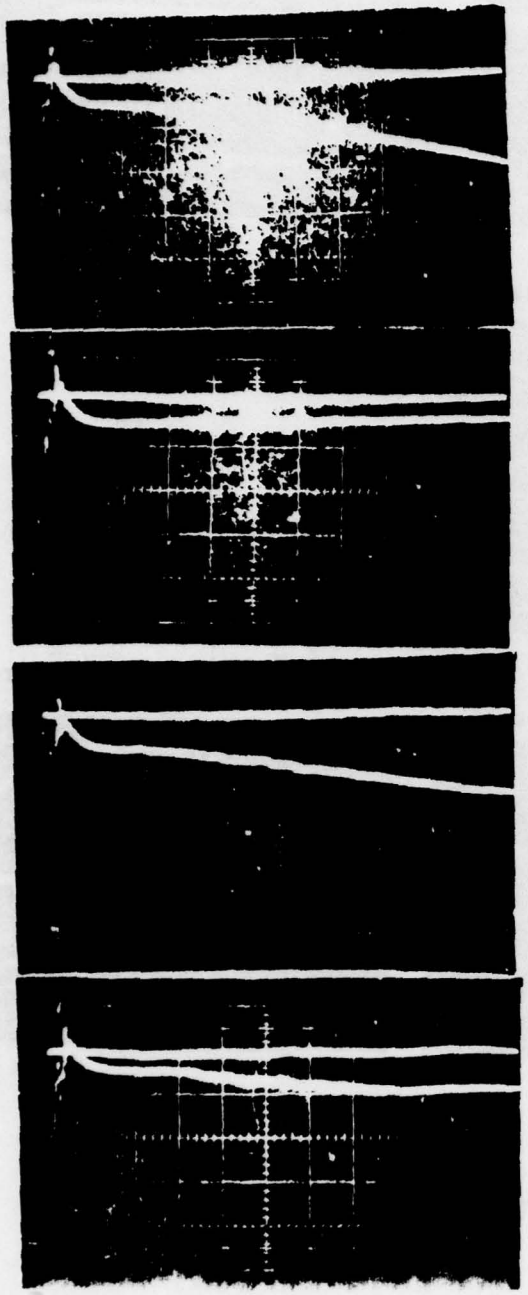

AF147-1 2 μsec/div λ = 4545

Shot No. 1
1.0 N.D. Filter
0.01 volts/division
2 sec/division

Shot No. 2

Shot No. 3

Shot No. 4